

Near-surface wind variability over the broader Adriatic region: insights from an ensemble of regional climate models

Andreina Belušić¹  · Maja Telišman Prtenjak¹ · Ivan Güttler² · Nikolina Ban³ · David Leutwyler³ · Christoph Schär³

Received: 17 March 2017 / Accepted: 26 August 2017 / Published online: 13 September 2017
© Springer-Verlag GmbH Germany 2017

Abstract Over the past few decades the horizontal resolution of regional climate models (RCMs) has steadily increased, leading to a better representation of small-scale topographic features and more details in simulating dynamical aspects, especially in coastal regions and over complex terrain. Due to its complex terrain, the broader Adriatic region represents a major challenge to state-of-the-art RCMs in simulating local wind systems realistically. The objective of this study is to identify the added value in near-surface wind due to the refined grid spacing of RCMs. For this purpose, we use a multi-model ensemble composed of CORDEX regional climate simulations at 0.11° and 0.44° grid spacing, forced by the ERA-Interim reanalysis, a COSMO convection-parameterizing simulation at 0.11° and a COSMO convection-resolving simulation at 0.02° grid spacing. Surface station observations from this region and satellite QuikSCAT data over the Adriatic Sea have been compared against daily output obtained from the available simulations. Both day-to-day wind and its frequency distribution are examined. The results indicate that the 0.44° RCMs rarely outperform ERA-Interim reanalysis, while the performance of the high-resolution simulations surpasses that of ERA-Interim. We also disclose that refining the grid spacing to a few km is needed to properly

capture the small-scale wind systems. Finally, we show that the simulations frequently yield the accurate angle of local wind regimes, such as for the Bora flow, but overestimate the associated wind magnitude. Finally, spectral analysis shows good agreement between measurements and simulations, indicating the correct temporal variability of the wind speed.

Keywords Adriatic region · CORDEX · Regional climate models · Convection-resolving models

1 Introduction

The CORDEX initiative is the latest effort in multi-model regional downscaling in a common experimental framework. This initiative aims to improve the understanding of regional and local climate phenomena, as well as their variability and changes. The CORDEX initiative started in 2009 and provides simulations at horizontal grid spacing of 0.44° (approximately 50 km) on various computational domains (Giorgi and Gutowski Jr. 2015). For the European (EURO-) and Mediterranean (MED-) CORDEX domains, additional simulations with grid spacing up to 0.11° (approximately 12.5 km) are provided for evaluation, historical periods, and climate scenarios. Recently, there has been a progression toward climate simulations with horizontal grid spacing up to 0.02° (approximately 2.2 km) (Prein et al. 2015), at which the parametrization of deep convection can be switched off (Weisman et al. 1997). The refined horizontal grid spacing allows two important questions regarding the added value of high-resolution RCM simulations to be addressed (Kotlarski et al. 2014; Rummukainen 2016). First, it is still not fully clear to what extent RCMs provide improved simulations (e.g. in terms of reducing systematic errors and/or providing more realistic details in simulating extreme events)

✉ Andreina Belušić
abelusic@gfz.hr

¹ Andrija Mohorovičić Geophysical Institute, Department of Geophysics, Faculty of Science, University of Zagreb, Zagreb, Croatia

² Meteorological and Hydrological Service of Croatia (DHMZ), Zagreb, Croatia

³ Institute for Atmospheric and Climate Science, ETH Zürich, Zürich, Switzerland

compared to global reanalysis or global climate models (GCMs). Second, how and where do the 0.11° simulations provide additional information to the 0.44° simulations?

For a range of regional and local flow phenomena, global reanalyses are not completely adequate tools because of their limited horizontal resolution (Sotillo et al. 2005; Feser et al. 2011; Menendez et al. 2014). Although global reanalyses (e.g., NCEP/NCAR reanalysis at a grid spacing of approximately 210 km or ERA-Interim reanalysis at approximately 80 km) and GCMs can effectively reproduce many large-scale climate features, they often fail in reproducing regional or local climate aspects (Rummukainen 2010). The improvement introduced by employing dynamical downscaling depends on various geographical factors, such as the complexity of the coastline and the representation of orography. For example, Sotillo et al. (2005) compared RCM to NCEP/NCAR reanalysis for several near-surface parameters and found larger improvements over the Mediterranean basin than over the Atlantic Ocean and for coastal buoys rather than open-ocean buoys. In a study comparing several RCMs and ERA-Interim reanalysis with QuikSCAT data, Herrmann et al. (2011) found that the shortcomings due to the low spatial reanalysis resolution are corrected in RCMs, but the temporal correlation with observations is to some extent smaller.

High-resolution simulations do not always offer a clear improvement compared to coarser-resolution simulations. For example, improvements in representing large-scale circulations (Di Luca et al. 2015) and seasonal means (Vautard et al. 2013) are not consistent and averaging over regional scales tends to cancel out the added value (e.g., in precipitation over the Alps, Torma et al. 2015). Nevertheless, the added value is pronounced on local scales where the capability to reliably represent small-scale events, such as extremes, increases with resolution (Herrmann et al. 2011; Giorgi et al. 2016). Furthermore, the increased resolution leads to a better representation of spatial distribution and intensities of local characteristics in daily precipitation and temperature amplitudes (Mayer et al. 2015; Torma et al. 2015), which depend on the interaction between fine-scale orography and atmospheric circulation. Similar improvements have been found for the representation of precipitation in the European Alps. As Torma et al. (2015) show, upscaling 0.11° simulations to a coarser grid spacing (0.44°) yielded added value, while the disaggregation of 0.44° simulations to a higher grid spacing (0.11°) did not show consistent improvements in the spatial pattern. This result implies that the added value has a physical basis, enabled by the finer topography obtained in the high-resolution simulations.

The improvements of the refined resolution are particularly pronounced in coastal (Vautard et al. 2013; Gütler et al. 2015) and mountainous (Ban et al. 2014; Prein et al. 2016; Rummukainen 2016) regions. Ban et al. (2014,

2015) validated COSMO simulations at 0.11° and 0.02° in terms of temperature and precipitation. They found that for daily statistics, both simulations perform rather well. However for hourly precipitation substantial differences can be found between the two simulations. While the simulation at 0.11° underestimates heavy and overestimates weak precipitation, the 0.02° simulation shows good agreement with observations and improves the timing of the diurnal cycle of precipitation.

Previous studies on dynamically downscaled climate simulations mostly focus on present-day temperature and precipitation, as well as their extremes and future changes (Branković et al. 2013; Ban et al. 2015). Near-surface wind has so far typically been assessed for seasonal offshore wind patterns and for area-averaged values (e.g., over the Mediterranean region in Herrmann et al. 2011). The Mediterranean region represents a significant challenge to state-of-the-art RCMs in realistically simulating local wind flows, due to the complex topography and the intertwined coastlines. A few studies that compared RCM wind fields to reanalysis data suggest that RCMs show lower biases and root-mean-square errors (*RMSE*) in comparison to reanalysis, particularly for coastal buoys (Sotillo et al. 2005; Winterfeldt and Weisse 2009). Furthermore Menendez et al. (2014) showed that higher resolution simulations provide a better fit in terms of a higher temporal correlation coefficient and a smaller *RMSE* in regions influenced by the nearby land. However, Herrmann et al. (2011) found that, when considering basin-averaged metrics, the differences between 50 and 10 km grid spacing simulations are not significant (less than 1%). They argue that large differences occur locally in regions of intense winds. In regions where wind channelling and influence of the topography is strong (e.g., Pyrenees, Alps, Greek mountains, Aegean islands), the spatial variability of wind speed and the spatial correlation of intense winds are significantly improved (up to 15%).

Since, in recent studies, analysis are often presented in terms of domain-averaged metrics (Vautard et al. 2013), the local geographically induced flows are smoothed out and neglected. An exception is the recent study by Obermann et al. (2016), which focuses on intense local phenomena, Mistral and Tramontane winds, that occur over southern France and the northwestern Mediterranean Sea. They show that the applied RCMs are able to correctly simulate Mistral and Tramontane situations, provided that the large-scale forcing is well represented in the driving model. However, during these events, most simulations underestimate wind speed over the Mediterranean Sea, but show smaller biases than coarse-resolution simulations and ERA-Interim.

In this study, we focus on the broader Adriatic region (Fig. 1), where the majority of the region is characterized by complex topography and steep terrain slopes. Particularly characteristic topographic features are the Dinarides,

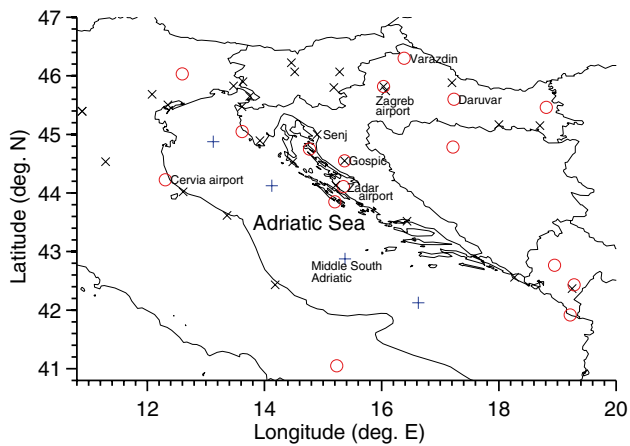


Fig. 1 Adriatic domain: spatial distribution of 47 stations selected from NCDC-NOAA database, DHMZ database and Crocontrol (HKZP) database. The stations were selected in order to be representative at the daily scale (5 out of 8 records per day have to exist) and representative of the period 1996/2001–2008 (at least 70% of daily data have to exist in the period of interest). The stations covering the period 1996–2008 are denoted by *black cross symbol*, those covering the period 2001–2008 by *red circle* and QuikSCAT data covering the period 2000–2008 are denoted by *blue plus symbol*. If there are two symbols at the same location, the time series was available from different sources with different lengths. Names appear for stations that will be discussed later in text

which span from northwest to southeast and separate the narrow eastern coastal region from the inland lowlands. Along the Adriatic coast, the most typical winds are Bora (experiencing strong influence of the terrain and usually perpendicular to the Dinarides; Grisogono and Belušić 2009), Sirocco (usually parallel to the coastline and mostly during the wintertime; Horvath et al. 2008), Etesian and sea/land breezes (dominantly in the warm part of the year; Prtenjak et al. 2010a, b). So far, the wind field characteristics over the Adriatic have mainly been investigated in studies focusing on numerical weather prediction simulations (Cavaleri et al. 1996; Horvath et al. 2011), on statistical downscaling of reanalysis (Heimann 2001), on global climate models (Pasarić and Orlić 2004) and on future wind power potential (Pašičko et al. 2012). However, to our knowledge, there are no climate studies that evaluate wind fields in RCMs on time scales longer than 10 years. To complement the existing studies, we assess the near-surface wind over the broader Adriatic region, evaluating the offshore and onshore near-surface wind climatology in RCM simulations with land-based observations and satellite data.

2 Data and methods

2.1 Climate model data

Seven EURO-CORDEX (Jacob et al. 2013), three MED-CORDEX (Somot et al. 2011; Ruti et al. 2016) and two additional simulations, provided by ETH Zürich, were considered (Table 1), all fully covering the analysis domain (Fig. 1). For the EURO-CORDEX simulations, the mean daily climate model data of the two 10 m wind components (u , v) and of the 10 m wind magnitude are used. For SMHI-RCA4 and DHMZ-RegCM42, sub-daily snapshots are available every 3 h. The MED-CORDEX dataset currently only has 10 m wind magnitude data for all three models. Depending on the model chosen, the simulations are 20–30 years long, but they all extend to 2008. The simulations employ a horizontal grid spacing of 0.11° (or 12.5 km), and they all have a corresponding coarser partner simulation at 0.44° (or 50 km). For initial conditions, lateral boundary conditions and sea surface temperatures ERA-Interim reanalysis (Dee et al. 2011) is used, since it is considered to be of very high quality (Brands et al. 2013). To complete the ensemble, we have acquired two simulations performed at ETH Zürich (ETHZ): ETHZ-CCLM-11 (COSMO convection-parametrizing model at 0.11°) and ETHZ-CCLM-02 (COSMO convection-resolving model at 0.02°), with snapshots available every hour. These simulations are 10 years long, extending from 1999 to 2008, and are performed using a two-step one-way nesting technique, dynamically downscaling ERA-Interim to 0.11° and then further to 0.02° .

Following the CORDEX protocol, none of the models presented use spectral nudging (Table 1). Throughout this study, the individual simulations will be identified by the abbreviation of the institution performing the simulation (see Table 1), plus the model name and horizontal grid spacing (02 for 0.02° , 11 for 0.11° and 44 for 0.44°).

2.2 Station observations

The broader Adriatic domain fully covers Croatia, Slovenia, Bosnia and Herzegovina, Montenegro, part of Italy and parts of other neighbouring countries (Fig. 1). Since for the selected domain no high quality gridded wind product over land is available, observed station-based wind magnitude and wind direction were utilized. Wind observations at 10 m above ground level from 1996/2001 to 2008 were obtained from NCDC-NOAA land-based stations (Smith et al. 2011), from the DHMZ database and from the Crocontrol (HKZP) database in SYNOP format. The NCDC-NOAA database performed a quality check before the data were released (<https://www.ncdc.noaa.gov/isd>) and wind data from Croatian institutions were controlled by the responsible persons

Table 1 Overview of the analysed models

Model	Institution (abbreviation)	1st vertical level height (m)	Spectral nudging	Analysed period
EURO-CORDEX				
CCLM4 (Rockel et al. 2008)	Climate Limited-area Modelling Community (CLMcom)	20	No	1996–2008
HIRHAM5 (Christensen et al. 2006)	Danish Meteorological Institute (DMI)	34	No	1996–2008
WRF331F (Skamarock et al. 2008)	Institute Pierre Simon Laplace/Institut National del' Environnement Industriel et des Risques (IPSL/INERIS)	40	–	1996–2008
RACMO22E (Van Meijgaard et al. 2008)	Royal Netherlands Meteorological Institute (KNMI)	10	No	1996–2008
RCA4 (Samuelsson et al. 2011)	Swedish Meteorological and Hydrological Institute (SMHI)	30	No (in buffer zone only)	1996–2008
ALADIN53 (Colin et al. 2010)	Centre National de Recherches Meteorologiques (CNRM)	30	No	1996–2008
RegCM42 (Giorgi et al. 2012)	Meteorological and Hydrological Service of Croatia (DHMZ)	40	No (in buffer zone only)	1996–2008
MED-CORDEX				
ALADIN52 (Colin et al. 2010)	Centre National de Recherches Meteorologiques (CNRM)	30	No	1996–2008
RegCM43 (Giorgi et al. 2012)	International Centre for Theoretical Physics (ICTP)	40	No	1996–2008
PROMES (Domínguez et al. 2010)	Universidad de Castilla-La Mancha (UCLM)	10	No	1996–2008
ETHZ				
CCLM (Leutwyler et al. 2016; 2017)	Swiss Federal Institute of Technology (ETHZ)	20	No	2001–2008

from the mentioned institutions. Afterwards, only a simple quality check was performed on daily data.

A station's daily mean value was used only if at least 5 out of 8 daily SYNOP snapshots were available for a specific day, and only for those stations that afterwards have daily means available for more than 70% of days in the period of interest. A small change in these criteria thresholds does not affect the spatial structure of the selected stations. Ultimately, a subset of 43 stations satisfied the criteria for both wind magnitude and direction. In this study, we consider stations less than 20 km from the coast as coastal stations, and the rest of the stations as inland stations (21 coastal and 22 inland stations).

2.3 QuikSCAT satellite observations

To obtain wind observations over the sea/ocean, we used gridded products of SeaWinds instruments measurements from the QuikSCAT satellite (hereafter, QuikSCAT), with a horizontal resolution of 25 km (Perry 2001; Ruti et al. 2008). Although available for the entire period of 2001–2008, the availability is limited by the cloud cover and by the daily passage frequency of the satellite over the Adriatic. Therefore, the daily mean was calculated from at most

two available raw data. As Herrmann et al. (2011) noted, QuikSCAT slightly underestimates weak and overestimates strong daily wind speeds when compared with buoy data. Furthermore, QuikSCAT measurements are of reduced quality for low wind speeds (<3 m/s) and close to the coastlines (Tang et al. 2004; Prtenjak et al. 2010b). Despite these shortcomings, QuikSCAT data correctly represents daily wind speed variability and have proven to be effective compared with offshore wind observations (Accadia et al. 2007). For the comparison with RCMs, we select four open-sea locations over the Adriatic with the largest number of available QuikSCAT daily data in the period of interest.

2.4 ERA-Interim reanalysis data

We have chosen to take two types of reanalysis products: the analysis product at time step 0 (ERA-Interim) and the prognostic product at time step 6 and 12 (ERA-Interim6). For example, on any specific day, the wind speed at 06:00 UTC is the analysis product at 06:00 UTC (time step 0; hereafter, ERA-Interim) or alternatively, is the result of the 00:00 UTC ERA-Interim simulation 6 h into the future (time step 6; hereafter, ERA-Interim6). In other words, ERA-Interim6 refers to a 6 and 12 h forecasts, initialized by the 00:00 and

12:00 ERA-Interim analysis. This approach allows testing of the robustness of our results to the underlying reference dataset and enables us to explore the impact of the initial conditions used in the ERA-Interim. It is important to note that ERA-Interim reanalysis does not assimilate wind data from land-based stations but assimilates the QuikSCAT data over oceans (from 2000, Dee et al. 2011).

2.5 Methods

The evaluation for the present-day climate simulations is performed from the daily data for most of the validation methods. There are numerous spatial interpolation methods available, and using some interpolation schemes may lead to spurious results. To avoid misleading results and to test for robustness, we employed two interpolation techniques, similar to Di Luca et al. (2015). To evaluate the wind climatology, first, the nearest neighbour (NN) approach was used. In this approach, the daily climatology at the nearest model grid point was linked to the daily time series of the land-based station. The second approach was bilinear interpolation (BI), where the weighted mean of the four closest grid points was calculated and compared to the observed time series.

Following Pryor et al. (2012), we perform upscaling of the 0.11° simulations to the 0.44° grid. The approach allows added value to be attributed to a better representation of physical processes (i.e., orographically induced wind flows; Torma et al. 2015). The upscaled simulations will be identified by the abbreviation “UPS”, along with the institution’s abbreviation and the model name.

The following standard skill scores were estimated: bias (simulations-measurements), standard deviation, root mean-square deviation (*RMSD*) and temporal correlation between observed and simulated series. In the resulting analysis a simulation is more successful when (i) the *RMSD* is smaller than the observed standard deviation and (ii) the simulation-based and measured standard deviations are comparable (Pielke 2002). Subsequently, *RMSD*, standard deviations and temporal correlation coefficients are summarized with Taylor diagrams (Taylor 2001) and are complemented by probability density estimates (PDEs), quantile–quantile (QQ) plots and wind roses.

We performed two statistical tests, namely, the Wilcoxon rank sum test and the 2D Kolmogorov–Smirnov test. The Wilcoxon rank sum test (WRS, Gibbons and Chakraborti 2011) is designed to test whether observed and simulated data series, here wind components and magnitude, are samples from continuous distributions with equal medians (null hypothesis) against the alternative hypothesis that they are not. The test assumes that the observed and simulated samples are independent. The 2D Kolmogorov–Smirnov test (Peacock 1983; Gibbons and Chakraborti 2011) is a

statistical test used to determine whether two 2D sets of data (e.g., u and v wind components) arise from the same or from different distributions. Here the null hypothesis is that simulated and observed wind components were drawn from the same 2D continuous distribution.

Additionally, the measure-oriented Brier skill score (*BSS*) and a distribution-oriented Perkins skill score (*PSS*) are used. *BSS* is utilized to test to what extent the RCM wind gives a better representation of measured wind than the ERA-Interim reanalysis. Here, we use the modified *BSS* following Winterfeldt et al. (2011) and Menendez et al. (2014):

$$BSS = \begin{cases} 1 - \frac{\sigma_D^2}{\sigma_R^2} & \text{if } \sigma_D^2 \leq \sigma_R^2 \\ \frac{\sigma_R^2}{\sigma_D^2} - 1 & \text{if } \sigma_D^2 > \sigma_R^2 \end{cases} \quad (1)$$

where σ_D^2 and σ_R^2 represent the error variances of the dynamically downscaled RCM (D) and reanalysis (R) respectively. The error variances are computed relative to the observations. Following this definition, the modified *BSS* can vary between -1 (reanalysis exactly matches the observations) and 1 (RCM exactly matches the observations). Negative values indicate a better reanalysis performance, while positive values indicate added value of the RCM in comparison to ERA-Interim reanalysis.

PSS, as defined by Perkins et al. (2007), measures a similarity between two PDEs. This metric calculates the cumulative minimum value of two distributions in each bin by measuring the common area between two PDEs. The bin centres are defined from observations. If a model simulates the observed conditions perfectly, the *PSS* is 1, which equals the total sum of the probability in a given PDE. Following Perkins et al. (2007), *PSS* is given by

$$PSS = \sum_1^N \min(Z_d, Z_o), \quad (2)$$

where N is the number of bins used to calculate the PDE, Z_d is the frequency of values in a given bin from the RCM distribution, and Z_o is the frequency of values in a corresponding bin from the observed wind distribution (the bin width is variable, but the number of bins is the same, independent of the analysed location).

In addition, the skill scores are complemented by Empirical Orthogonal Function (EOF) analysis (Ludwig et al. 2004) and spectral analysis (Žagar et al. 2006; Horvath et al. 2011). The power spectra are calculated only for the simulations that have sub-daily data available and only for stations where less than 10% of the SYNOP data are missing for the period 2001–2008. After applying these criteria, 6 out of 47 stations are left for spectral analysis. Since spectral analysis requires a continuous time series, the gaps from the

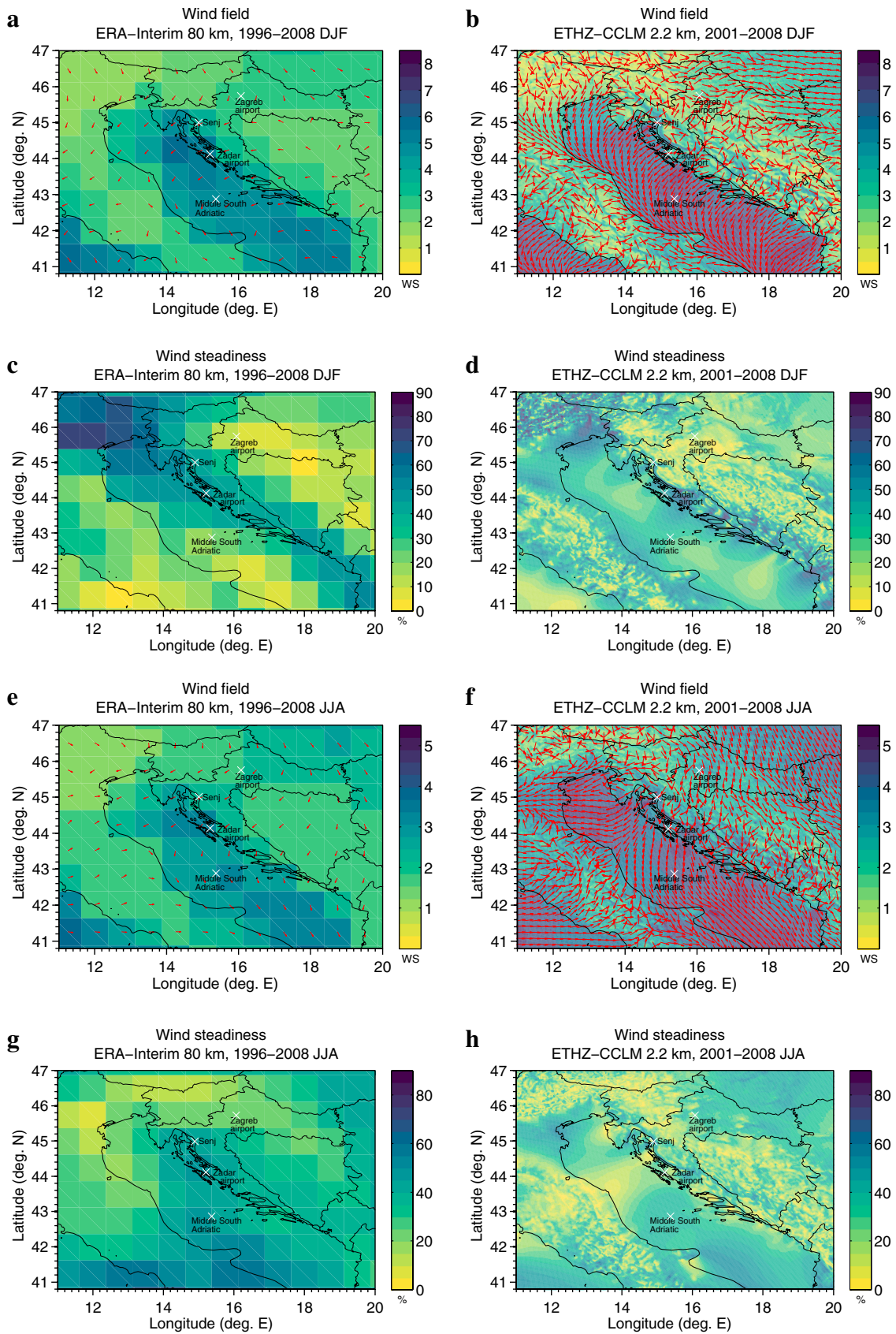


Fig. 2 (*Top panels*) winter season (DJF) and (*bottom panels*) summer season (JJA) wind field and persistence in the Adriatic domain for ERA-Interim (*left column*) and ETHZ-CCLM-02 (*right column*). The wind field is presented as mean vectors (*vectors*) and the mean scalar wind speeds (*colours*) for the periods shown in Table 1. *Arrows* are normalized and denote only the wind direction. The wind steadiness is a non-dimensional parameter defined as the ratio between mean vector and scalar wind speed ranging from 0 (low wind direction persistency) to 100% (fixed wind direction in time) which allows detection of dominant persistent wind regimes. The *white symbols* denote 4 region representatives

remaining missing data were filled with linear interpolation. The filled data samples are sporadic and random, do not appear in groups and therefore do not corrupt the time series. Also, due to the short length of the time series, we assume that the temporal variability is not substantially affected by the gap filling. After removing linear trends, power spectral density estimates of the 10 m wind magnitude were calculated using Welch's averaged modified periodogram method (Belušić and Güttler 2010; Večenaj et al. 2010). In this procedure, the half-overlapping window length was equal to 256 data points, and the sampling rate was 3 h.

3 Results and discussion

3.1 Spatial wind characteristics

Figure 2 displays the seasonal-mean (winter season-DJF and summer season-JJA) wind vectors, scalar wind speeds and wind steadiness over the Adriatic for ERA-Interim reanalysis (Fig. 2 first column, the lowest resolution available) and for the ETHZ-CCLM-02 simulation (Fig. 2 second column, the highest resolution available). The wind steadiness is a non-dimensional parameter defined here as the non-linearized ratio of the mean vector and scalar wind speed (Halpren 1979; Powell et al. 1995; Dunion et al. 2003) ranging from 0 (low wind direction persistency) to 100% (fixed wind direction in time), which allows the detection of dominant persistent wind regimes. The added value of dynamical downscaling to finer grid spacing can immediately be recognised from the much more detailed structures in the spatial wind patterns (Fig. 2).

In DJF and over the Croatian lowlands, the relatively weak northwesterly (NW) wind in ERA-Interim (Fig. 2a) does not deviate significantly from the prevailing westerly wind in ETHZ-CCLM-02 (Fig. 2b). Still, improvements can be seen in much finer wind structures (taking into account more variable wind intensity, direction and steadiness). They are evident over the entire mountainous ranges and in the vicinity of the isolated mountains in the lowlands. Regardless of the horizontal grid spacing, coastal and open-sea areas are characterized by northeasterly (NE) wind of

greater intensity and wind steadiness (>40%; Fig. 2a–d). In contrast to the relatively uniform wind field in the ERA-Interim reanalysis (Fig. 2a, c), ETHZ-CCLM-02 (Fig. 2b, d) simulates much more complex wind structures. Regions of the NE wind with greater speeds (Fig. 2b) overlap with regions of wind steadiness exceeding 60% (Fig. 2d) along the eastern Adriatic coast. They reveal the Bora jets, which are associated with coastal mountain passes, as observed in measurements and case-study simulations (Grisogono and Belušić 2009; Stiperski et al. 2012; Prtenjak et al. 2015). Opposite to the Bora wind, the Sirocco is not easily identifiable in the 10 m wind climatology (over the open sea). An indication is the low wind steadiness over the open-sea area (particularly southward from the Middle South Adriatic).

In the JJA season, which is less windy than the DJF season, the wind intensity differs less between land and open sea (Fig. 2e, f). Still, the wind speed over the sea is greater, revealing two dominant wind regimes. NE-E flow occurs in the northern part of domain and NW flow in the southern part (Etesian; with steadiness >60%), which strengthens towards the south. In the ETHZ-CCLM-02 simulation, larger variations in the coastal wind directions (Fig. 2f) as well as mostly low wind steadiness (<30%; Fig. 2h) indicate the presence of thermally-induced winds (sea/land breezes and slope winds) that alternate in wind direction within 24 h.

The seasonal wind climatology, especially from ETHZ-CCLM-02, corresponds well to the 10 m wind distribution obtained by the ALADIN model at 2 km grid spacing made by dynamical adaptation in Horvath et al. (2011) (see their Fig. 2) and QuikSCAT analysis in Accadia et al. (2007) (see their Fig. 3).

3.2 Model evaluation

Throughout this paper, improvements introduced by fine-resolution simulations will be quantified using various validation techniques. A detailed validation of the surface wind values against available observations was performed in time and space. First, a basic overview of all 47 stations is provided. According to Herrmann et al. (2011) and Menendez et al. (2014), the variability of the wind field over land is largely influenced by fine-scale topography, while the wind field over the open-sea is mostly affected by large-scale atmospheric circulations. Following their hypothesis, the wind field in the Adriatic experiences the influence of various terrain types, from the open-sea region, where the driving processes are mainly under the influence of large-scale motions and where the wind field is more uniform, to the coastal transition region, where topography plays a significant role in the wind field modifications, and to the inland region, where the wind field is again more homogeneous (see Fig. 2). Consistent with these studies, and with the wind characteristics discussed in Sect. 3.1, the stations

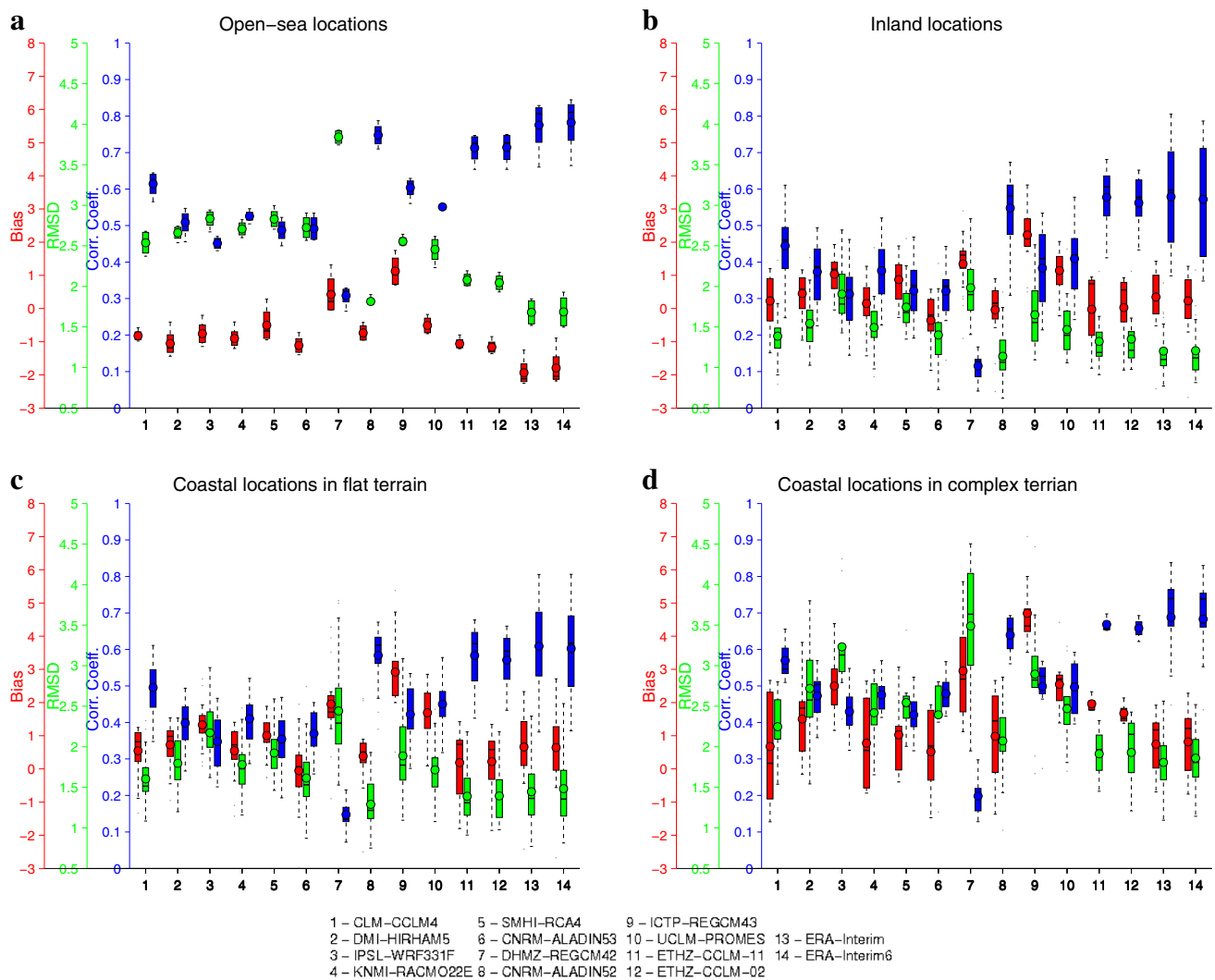


Fig. 3 Bias (red), *RMSD* (green) and correlation coefficient (blue) summarized for all 47 locations analysed. Each box represents a distribution where all the stations are integrated. The results are divided in three groups, namely **a** open-sea locations, **b** inland locations and **c**

are categorised into four main groups: open-sea locations, inland stations, coastal stations in relatively flat terrain and coastal stations in complex terrain with steep hinterland.

3.2.1 Conventional statistics in time and space

In Fig. 3, distributions of bias, *RMSD* and correlation coefficients for all 47 stations are presented by regions for a chosen set of simulations (i.e., ERA-Interim, 0.44°, 0.11° and 0.02° grid spacing). Therefore, each topographic group is presented separately and each station depicts a sample in the distribution. The biases over the open-sea region (Fig. 3a) are mostly negative, with the spread ranging from –2.5 to 2 m/s, depending on the particular location. This

locations in flat coastal terrain and **d** locations in complex coastal terrain. Numbers from 1 to 11 represent NN 0.11° simulations, number 12 is 0.02° NN simulation, as seen from the legend in the bottom

means that the wind speeds are underestimated in the simulations. In contrast, most of the biases over the inland stations are approximately zero or positive (in the range of –3 to 4 m/s, Fig. 3b), indicating overestimated wind speed in the simulations. Furthermore, while the biases for coastal stations in relatively flat terrain show similar characteristics (Fig. 3c) as further inland, the maximum biases in the complex coastal region (Fig. 3d) are two times larger than the other maximum biases. In the coastal terrain with steep hinterland, the values range from –2 to 8 m/s, indicating a large spread of biases among stations. This implies that refining the grid spacing to a few km is needed if we want to capture the small-scale low speed wind features and overcome well-known model limitations (e.g., insufficient discernment

by horizontal and vertical grids, too coarse topography and land-use representations, switching on/off of certain model parameterizations). The presented results also agree with Obermann et al. (2016) (see their Fig. 9), where the biases range from -3 to 2 m/s at open-sea and from -1 to 5 m/s over land.

The *RMSDs* are larger above sea and along the complex coastline (~ 2 – 3 m/s), where the wind intensity is high and smaller over the flat coastline and in the lowlands (1.5 – 2 m/s) (Figs. 2, 3). The correlation coefficients vary from region to region and between models, showing higher values above the open-sea region and steep coastline where the wind is more intense and, in some seasons, largely persistent.

Comparing only models, the biases and the spread in biases are lowest for ETHZ simulations and CNRM-ALADIN52, while they are largest for DHMZ-RegCM42 and ICTP-RegCM43 for all station locations. In terms of temporal correlation coefficients, the ETHZ simulations and ERA-Interim are close to each other, while the RegCM simulations show the smallest values. ERA-Interim and ERA-Interim6 show similar behaviour. Although the impact of the differences in these two ERA-Interim products may be relevant when analysing specific weather events, the similarities on the climatological time scale support the use of ERA-Interim only.

In the following section, the analysis will only be performed on stations representing the four main terrain types (see Sect. 3.2): the Middle South Adriatic (open-sea location), Zagreb airport (inland station), Zadar airport (station in the flat coastal terrain), and Senj (station in complex coastal terrain with steep hinterland). The Zadar and Senj areas are interesting because they are well-known Bora minimum (Stiperski et al. 2012) and Bora maximum (Prtenjak et al. 2015) sites, respectively (see also Fig. 2). The main criterion for the open-sea and inland stations was data availability.

Taylor diagrams in Fig. 4 are shown for all available simulations at 0.11° and 0.44° grid spacing for the four chosen locations. Since no substantial changes were found after upscaling, these results are not shown here. We present the open-sea location (Fig. 4a), the inland station (Fig. 4b), the station in the flat coastal terrain (Fig. 4c) and the station in the complex coastal terrain with steep hinterland (Fig. 4d). The largest *RMSD* can be found for the Zadar airport and Senj stations which are located in the coastal area, while the smallest can be found at the Zagreb airport station, located in the region without large terrain gradients.

The higher-resolution simulations have smaller errors compared to their coarser resolution partners. Smaller errors in fine grid spacing simulations over open-sea locations were also found by Herrmann et al. (2011). For the same terrain type, Obermann et al. (2016) found a better representation

of Mistral and Tramontane conditions in the western Mediterranean Sea when the grid spacing was refined. They also argued that the highest biases occur in the coastal area, an aspect we have also found for our locations depicted in Fig. 3.

The ERA-Interim reanalysis has the largest temporal correlation coefficient at all stations analysed, but it usually overestimates the measured standard deviation. Moreover, all four ERA-Interim time series show very similar behaviour, but the results are more sensitive to the horizontal interpolation technique chosen (NN or BI, see Sect. 2.5) than to the selection of ERA-Interim time series (based on the analysis or forecast for specific hours). Moreover, the differences between the interpolation approaches (NN or BI) in RCMs are negligible, which is particularly important for stations in complex terrain with steep hinterland. These results imply that the choice of RCM affects the final results much more than the choice of interpolation technique. From the CORDEX ensemble, CNRM-ALADIN53 appears to best fit the observations, being the closest to the normalized standard deviation line 1 at all stations and having the greatest temporal correlation coefficient. Still, for consecutive day-to-day events, all 0.11° CORDEX simulations exhibit similar results, having generally lower temporal correlation coefficient than ERA-Interim, but some simulations locally reduce the *RMSD* (i.e., for Zadar airport where the wind field throughout the year is very variable; see also Fig. 11). The lower temporal correlation may partly be explained by not using spectral nudging; allowing the model to more freely evolve in the inner domain. However, while spectral nudging can improve the correlation, it typically also decreases the variability (von Storch et al. 2000).

ETHZ-CCLM-11 and -02 show good performance, very close to that of ERA-Interim. The temporal correlation coefficient obtained from the ETHZ simulations is similar to ERA-Interim. Even if the temporal correlation coefficients are similar, the reasons for this feature may be different. First, the refinement in grid spacing may not lead to linear improvement in statistical parameters (seen also when refining from 50 to 12.5 km) (Ranjha et al. 2016). Second, while ERA-Interim assimilates the measurements, it has very coarse grid spacing, which does not permit the evolution of small-scale events (large *RMSD* for coastal stations). In contrast, the ETHZ-CCLM-02 simulation, with very fine spatial resolution, coherently resolves day-to-day events.

The DHMZ-RegCM42 simulation has the lowest temporal correlation coefficient for all stations (as in Fig. 3), but its *RMSD* does not deviate from those of other simulations. It is interesting to note that other studies (Turuncoglu and Sannino (2016) over the Mediterranean basin) found similar results. Turuncoglu and Sannino (2016) analysed the RegCM42 at 0.44° grid spacing coupled with the Regional Ocean Modeling System (ROMS) (called REGESM). They

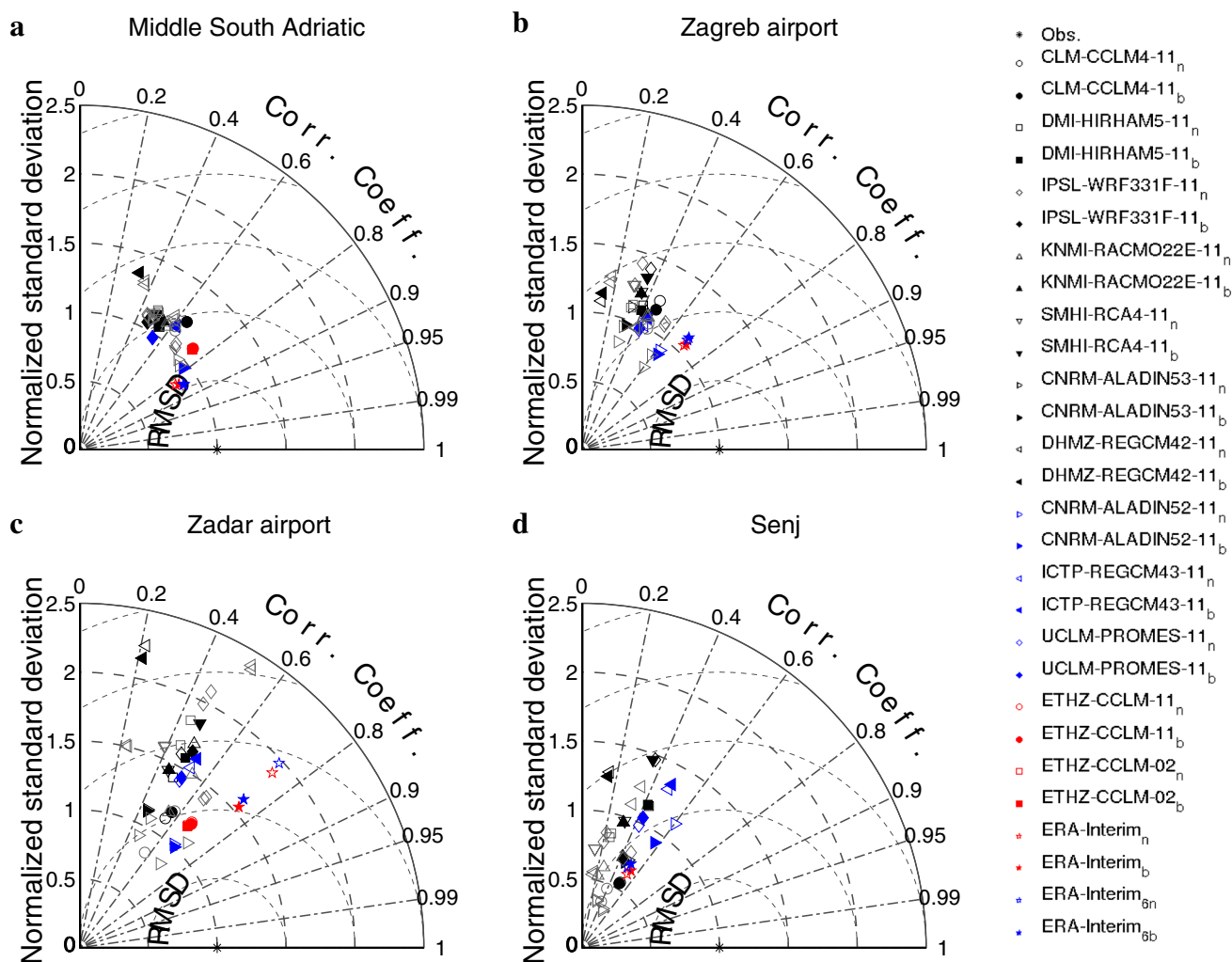


Fig. 4 Taylor diagrams exploring the model performance respect to the observed wind magnitude for: **a** an open-sea location (*Middle* South Adriatic), **b** inland location (Zagreb airport), **c** station in the flat coastal terrain (Zadar airport) and **d** station in the complex coastal terrain (Senj). The corresponding legend is to the right. *Non filled symbols: NN (n), filled symbols: BI (b), black symbols EURO-CORDEX, blue symbols MED-CORDEX, red symbols ETHZ simu-*

lations, red stars ERA-Interim, blue stars ERA-Interim6 prognostic, grey symbols 0.44° CORDEX simulations. The diagrams are normalized, so the distance from observations (1, 0 location) corresponds to normalized and centred root-mean-square difference, expressed as multiple of the observed standard deviation. The period studied: **a, c** 2001–2008, **b, d** 1996–2008

found that RegCM standalone and REGESM can reproduce quite well the wind direction when averaged over large area, but they have problems in reproducing wind field when compared to buoys. They argued that the reason lies in the coarse resolution, but our results showed that the 0.11° grid spacing simulation did not introduce any improvement. In our study, due to relatively poorer statistical indicators, additional sensitivity tests of DHMZ-RegCM42 were performed. The preliminary results showed a sensitivity of the temporal correlation to the choice of the model's parametrization schemes of the planetary boundary layer and deep convection (as shown also in Gómez-Navarro et al. 2015). However, further investigations are still needed to confirm these results.

In addition, Taylor diagrams for DJF and JJA are shown in Fig. 5 for the Zadar airport station (a coastal station) and for 0.11° simulations with NN interpolation only. Similar behaviour is found for the other three group representatives (not shown). The overestimation of the measured standard deviation is larger and the correlation coefficient is smaller in the summer (JJA) season (Fig. 5b) than in the winter (DJF) season (Fig. 5a), although the wind magnitude is larger in DJF than in JJA (Fig. 2). The seasonal pattern likely arises from day-to-day wind speed analysis, due to persistent large-scale flows typically found during DJF (Fig. 2), and more convective events and smaller-scale variability during JJA. The summer conditions are more difficult to reproduce

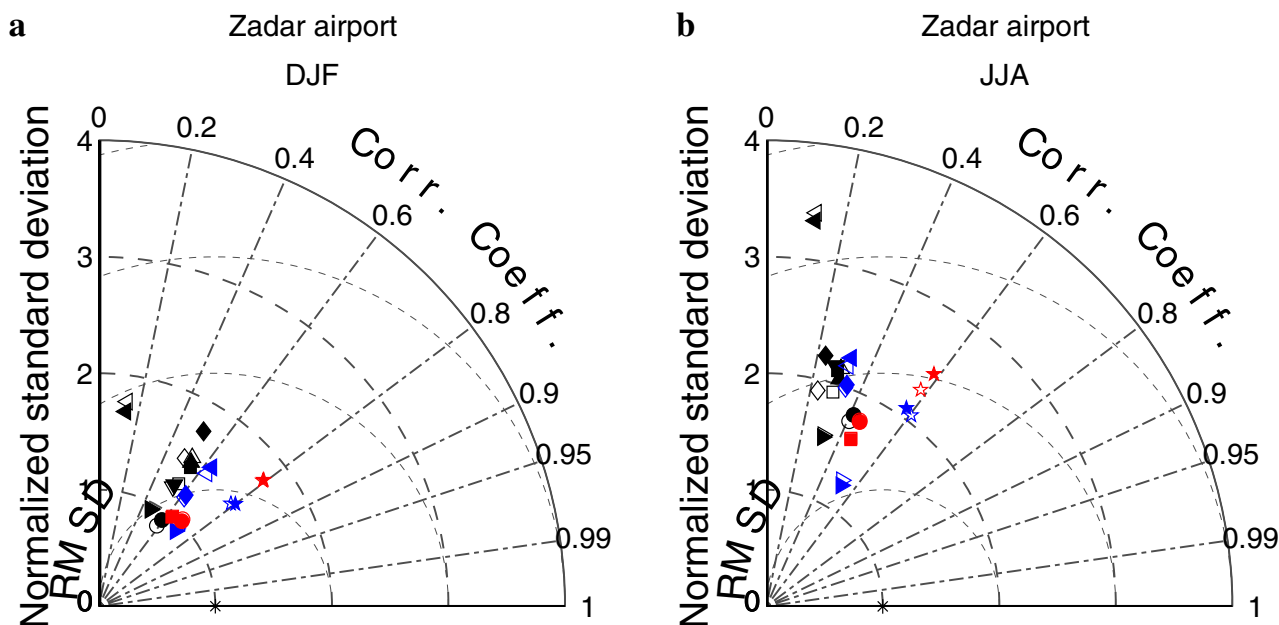


Fig. 5 Taylor diagrams exploring the seasonal pattern for wind magnitude at the Zadar airport station (Croatia, coastal station, 2001–2008) for **a** DJF and **b** JJA. The legend is the same as in Fig. 4, but only for NN interpolation

in RCMs and especially by ERA-Interim. This result is in line with previous studies, where it has been shown that numerical models typically reproduce weak flow conditions (<1.5 m/s) less accurately, particularly over the complex coastal terrain (Baklanov and Grisogono 2007; Prtenjak et al. 2010b).

Wind magnitude boxplots are presented for the same four representative locations (Fig. 6), showing how wind field characteristics vary with distance from the coast. In general, the differences between inland and coastline locations are quite well simulated. The maximum wind speed is higher near the Adriatic coast and drops moving inland. A larger simulation ensemble spread is found for the coastal station (as in Fig. 3), while the simulations at the inland station and open-sea location agree within the wind speed range. Both the inland station and open-sea location have small ensemble spread, but the inland station has its maximum magnitude at approximately 10 m/s and the open-sea location at approximately 25 m/s. The boxplots support the hypothesis that wind field characteristics exhibit more diverse features in complex topography.

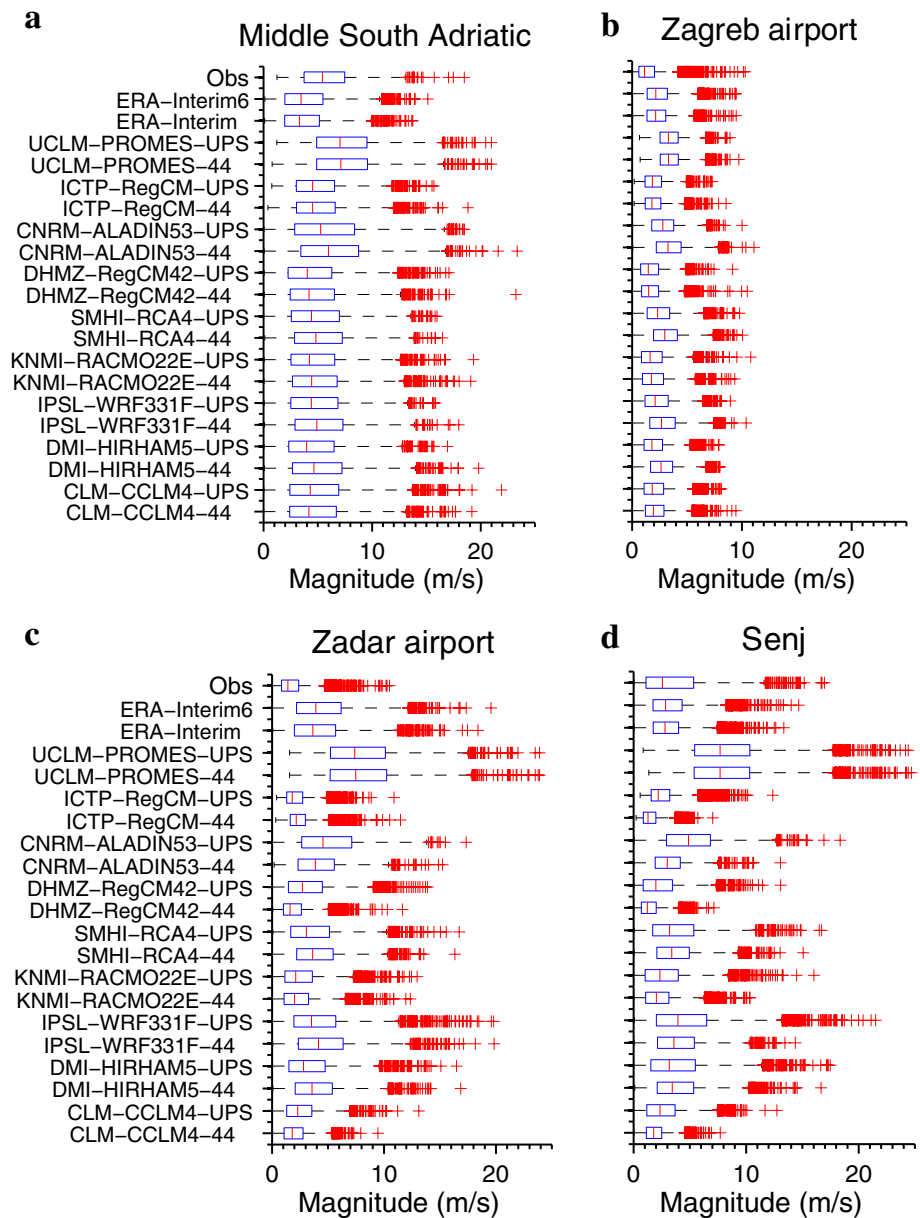
The analysis in Fig. 6 demonstrates substantial added value for the 0.11° simulations. Comparing both simulations from the same model (default and upscaled simulations), the median usually draws closer to the observations in the upscaled results of the 0.11° simulations, shifting the whole distribution closer to the observations. Actually the simulations with 0.11° grid spacing would be closest to the observed boxplots, but they are not shown here, since we want

to focus on the comparison between the upscaled and default 0.44° grid spacing.

Two statistical tests, 2D Kolmogorov–Smirnov and WRS, at the 10% significance level are almost always negative, rejecting the hypotheses that (a) the two independent samples (observations and simulation) arise from the same distributions and that (b) the two samples have the same median. In fact, none of the four region representatives used above (with NN interpolation) satisfy the null hypothesis of the 2D Kolmogorov–Smirnov test (not shown), and only at Senj is the WRS test positive for the ERA-Interim reanalysis. This finding is rather surprising and indicates that RCMs face difficulties in reproducing the observed 10 m wind components. We will come back to these results further below, when discussing an EOF analysis. Furthermore, we noticed that the median wind components are better simulated than the wind magnitude. Also, the WRS test showed that the median is to some extent better simulated for the DJF and JJA time series than it is for the entire period (not shown).

The benefits of dynamical downscaling, compared to ERA-Interim reanalysis, are further examined by wind magnitude QQ plots (Fig. 7). The results are shown only for the NN approach, since the conclusions are the same for BI. The results of the QQ analysis confirm the benefits of the dynamical downscaling approach in the coastal area, especially in the region with complex topography (Senj) and for extreme wind events (as in Sotillo et al. 2005; Herrman et al. 2011). Similar to the analysis discussed above, the open-sea location and the inland station have a smaller

Fig. 6 Wind magnitude boxplot comparison at 0.44° resolution for the NN approach at **a** open-sea location (*Middle South Adriatic*), **b** inland station (Zagreb airport), **c** station in the flat coastal terrain (Zadar airport) and **d** station in the complex coastal terrain (Senj). The *box* represents the range from 25th (P25) to 75th (P75) percentile, the *red line* is the median, the *red crosses* are the outliers defined as higher than $P75 + 1.5 (P75 - P25)$ or smaller than $P25 - 1.5 (P75 - P25)$. The period studied: **a, c** 2001–2008, **b, d** 1996–2008



ensemble spread but display a systematic underestimation of small wind speeds for the open-sea location (as in Herrman et al. 2011) and a systematic overestimation for the inland station. For the flat coastal stations, on the other hand, all simulations overestimate wind magnitude for all ranges of wind speed. However, for Senj, no clear grouping (underestimation or overestimation) dominates in the ensemble. The largest discrepancies in the coarse-resolution simulations are found in coastal areas for strong winds associated with regional wind patterns (i.e., Bora and Sirocco). Here the added value of the high-resolution dynamical downscaling is the most evident (see also Fig. 2).

The improvements at 0.11° grid spacing at the open-sea location and for the inland station are not visible, and

already the ERA-Interim time series (denoted with blue stars) shows a good agreement with observations. For the two coastal stations, the added value of the dynamical downscaling becomes more evident, and the differences among coarser-resolution reanalysis, 0.44° simulations and 0.11° grid spacing simulations become larger. Overall, the ETHZ simulations (denoted in red) are the closest to the diagonal line, and it seems that upscaling the 0.11° simulation to 0.44° (second column) yields a small improvement.

3.2.2 Skill scores

For further assessment of the added value with respect to ERA-Interim, the modified *BSS* of ERA-Interim and of the

RCM simulations are computed (Figs. 8, 9). Since the Taylor diagram (Fig. 4) already showed that the ERA-Interim results are affected by the interpolation technique, the results for both the NN and BI approaches are displayed. A sensitivity to the chosen interpolation approach can be also seen, e.g., in Fig. 8c for the ETHZ-CCLM-11 and -02 simulations. For these simulations, the NN approach shows a 30% larger modified BSS than the BI approach. The comparison between the upscaled 0.11° and 0.44° simulations is not consistent in the case of the modified BSS.

Over the open-sea (Fig. 8a) and over the inland region (Fig. 8b), where ERA-Interim can capture the sea-land mask and topography well, the vast majority of RCMs still cannot outperform the modified BSS of the reanalysis. The modified BSS is very high and negative, which is consistent with Menendez et al. (2014). Over the open-sea location (Fig. 8a), the CNRM-ALADIN53 and ETHZ simulations have a positive modified BSS. For the coastal stations (Zadar airport and Senj), the modified BSS does not indicate consistent added value for the RCMs. Although the modified BSS has more positive values for higher-resolution RCMs in the case of Zadar airport, negative values dominate in Senj. Several factors contribute to this result. First, for the Senj location, the corresponding model point is classified as a land point in the ERA-Interim land-sea mask. This is not the case for the Zadar airport location, where the corresponding model point is considered a sea point. This misrepresentation leads to, e.g., higher-than-observed wind speeds in ERA-Interim (Fig. 6c). In addition, the wind above Senj station has very high persistence (Fig. 2) due to the NE wind (Bora) during the whole year, which was indicated by Poje (1992). Several factors influence the Bora formation, including the position of the large-scale pressure systems and the height of the surrounding orography. Since ERA-Interim can reproduce the large-scale motions correctly and because the topography is reasonably well captured for this feature, the persistent NE flow at Senj station is successfully captured (see also Fig. 12). Thus, there is no possibility for the RCMs to outperform the reanalysis. Winterfeldt and Weisse (2009) also did not find evident added value when computing the modified BSS for RCM at a 0.44° grid spacing and NCEP/NCAR reanalysis over the northeast Atlantic and North Sea. However, they find a statistically significant improvement in complex coastal areas and in frequency distribution. In contrast, the wind is more variable during the year at the Zadar airport station (Fig. 2), and the added value of RCMs, in terms of modified BSS, is pronounced. For open-sea locations, we find that the majority of 0.11° and 0.44° simulations (except the ETHZ simulations and CNRM-ALADIN53) did not add any value to the ERA-Interim simulations. It could be argued that this is due to the assimilation of QuikSCAT data in ERA-Interim reanalysis. Still, Feser et al. (2011) noted that the modified BSS at the open-ocean is independent of the

assimilation of near-surface wind observations, although the reanalysis assimilates near-surface winds.

The modified BSS has also a clear seasonal dependence, having larger values during DJF than JJA, as illustrated for two stations for 0.11° and the NN technique in Fig. 9. The same applies for other stations (not shown). From this analysis we conclude that the added value of dynamical downscaling in coastal terrain (Fig. 9a, Zadar airport, Croatia) is fairly effective, particularly for the DJF season.

The evaluation based on the skill scores discussed above appears to be contradictory. The modified BSS is dependent on the daily temporal coherence. Hence we find that the added value in terms of temporal correlation is not sufficiently pronounced for all simulations. To preserve the correlation in time, e.g., re-initializations for each simulated day, or several times per day, would be needed. We can note that the distribution-dependent PSS (Fig. 10) gives more consistent results. RCMs are intended to simulate the statistics correctly, and the PSS quantifies how well RCMs fulfil this aim. Consequently, we expect RCMs to have a higher PSS than ERA-Interim. Since PSS only slightly depends on the interpolation technique used, the BI result will be omitted here. The PSS for the 0.11° (and 0.02°) grid spacing simulations using the NN approach is analysed in Fig. 10.

In contrast to the results found for the modified BSS, the PSS results (Fig. 10) lead to the conclusion that all simulations are quite successful in simulating the PDE. We do not find any substantial differences between inland and coastal regions. The two ETHZ simulations no longer stand out from the CORDEX group, but they still have larger PSS values than the ERA-Interim reanalysis (both ERA-Interim and ERA-Interim6 time series). In general, the score is the highest at the open-sea location, and the spread of the PSS range is smaller than for the other two regions, implying that they are the easiest to represent, since the motions are mostly affected by the large-scale circulation (Winterfeldt and Weisse 2009). However, it is surprising that the same result also applies for the Adriatic Sea, which is a quite narrow semi-open sea that is highly influenced by the surrounding mountain ranges. Also consistent is the performance of ICTP-RegCM43 and DHMZ-RegCM42 which have the lowest PSS at almost all locations. The 0.11° and upscaled simulations have a slightly higher PSS than the corresponding 0.44° simulations.

3.2.3 Wind rose and EOF analysis

Wind roses are used to investigate the wind field's frequency and angular distribution. For coastal stations in the Adriatic coast they are particularly insightful, since these stations are under the influence of severe winds (i.e., Bora and Sirocco). Figure 11 shows the wind rose for the NN approach at the Zadar airport station. At this station, all typical winds are

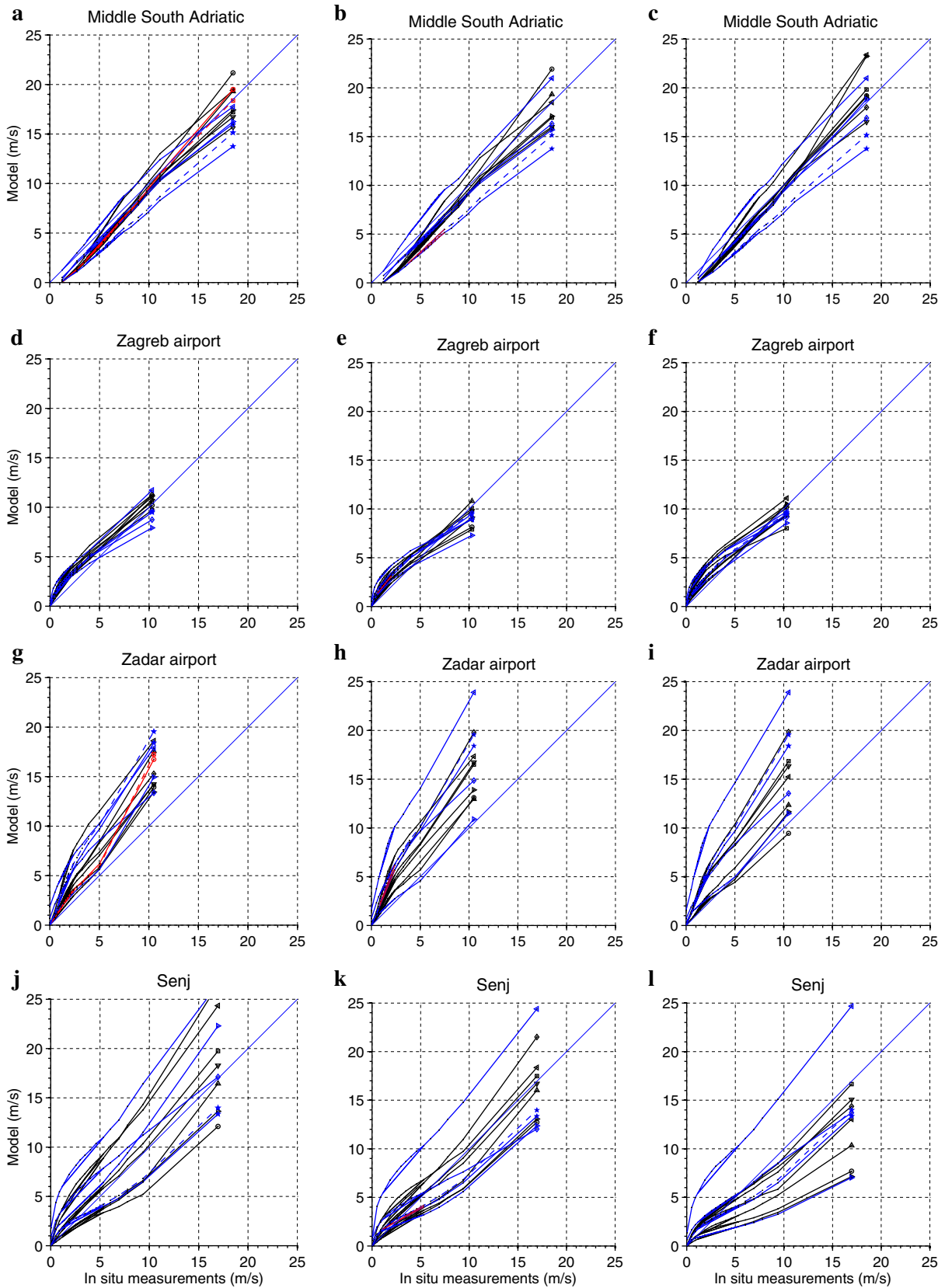


Fig. 7 QQ plots of wind magnitude for **a–c** open-sea location (*Middle South Adriatic*, 2001–2008), **d–f** inland station (Zagreb airport, 1996–2008), **g–i** station in the flat coastal terrain (Zadar airport, 2001–2008) and **j–l** station in the complex coastal terrain (Senj, 1996–2008) extracted using NN method. *First column (a, d, g):* 0.11° simulations, *second column (b, e, h):* upscaled 0.11°–0.44° simulations and *third column (c, f, i):* 0.44°. *Diagonal line* represents the 1–1 relationship. EUR-CORDEX simulation are in *black*, MED-CORDEX in *blue*, ETHZ-CCLM-11 in *solid red*, ETHZ-CCLM-02 in *dashed red*, ERA-Interim in *solid blue* and ERA-Interim6 in *dashed blue*. Symbols are the same as for Fig. 4. QQ lines are plotted using every 10-th percentile for values smaller than median and every 5-th percentile for values larger than median

equally represented, and the Bora wind speeds are typically small. The wind roses contain a CORDEX group member representative at 0.11° (Fig. 11d), 0.44° (Fig. 11f), the upscaled resolution (Fig. 11e), the ETHZ simulations at 0.11° (Fig. 11c) and 0.02° (Fig. 11b) and, finally the ERA-Interim simulation (Fig. 11g). While ETHZ-CCLM-02 clearly agrees the best in terms of wind direction frequencies, it overestimates the wind magnitude, especially for higher wind speeds. However, it captures the Bora direction (NE) and Sirocco direction (SE) quite well. The corresponding 0.11° simulation (ETHZ-CCLM-11) also captures the Bora wind and while it agrees better on the wind magnitude,

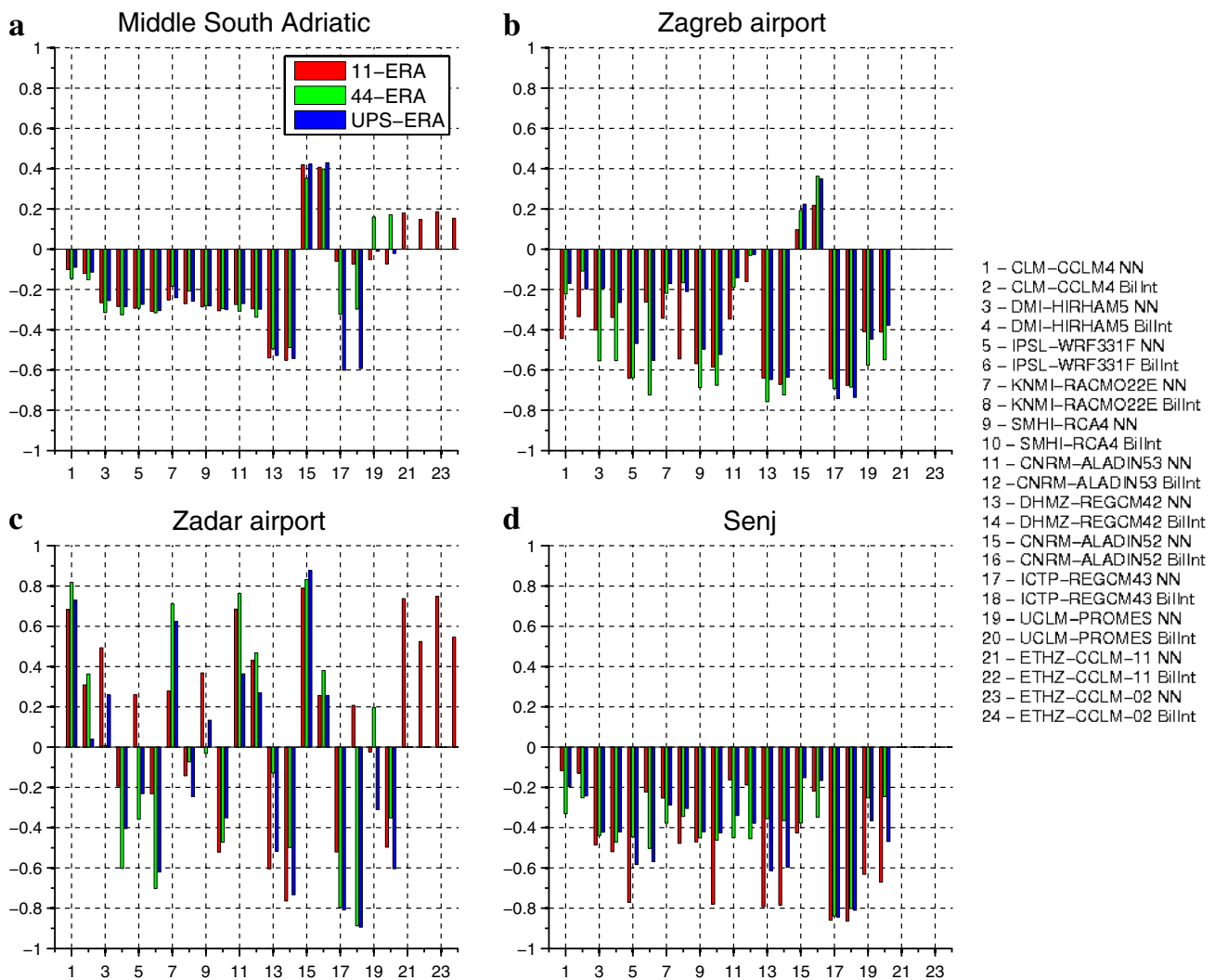


Fig. 8 The modified BSS for **a** an open-sea location (*Middle South Adriatic*), **b** inland station (Zagreb airport), two coastal stations **c** Zadar airport and **d** Senj. BSS shown is the one calculated with ERA-Interim analysis data series. *Each number on x-axis* represents a simulation corresponding to the legend to the right. *First bar:* BSS for

0.11° (or 0.02° for ETHZ) simulation, *second bar:* 0.44° simulations and *third bar:* upscaled 0.11°–0.44° simulations. ETHZ simulations (when available) have 0.11° and 0.02° resolution. The period studied: **a, c** 2001–2008, **b, d** 1996–2008

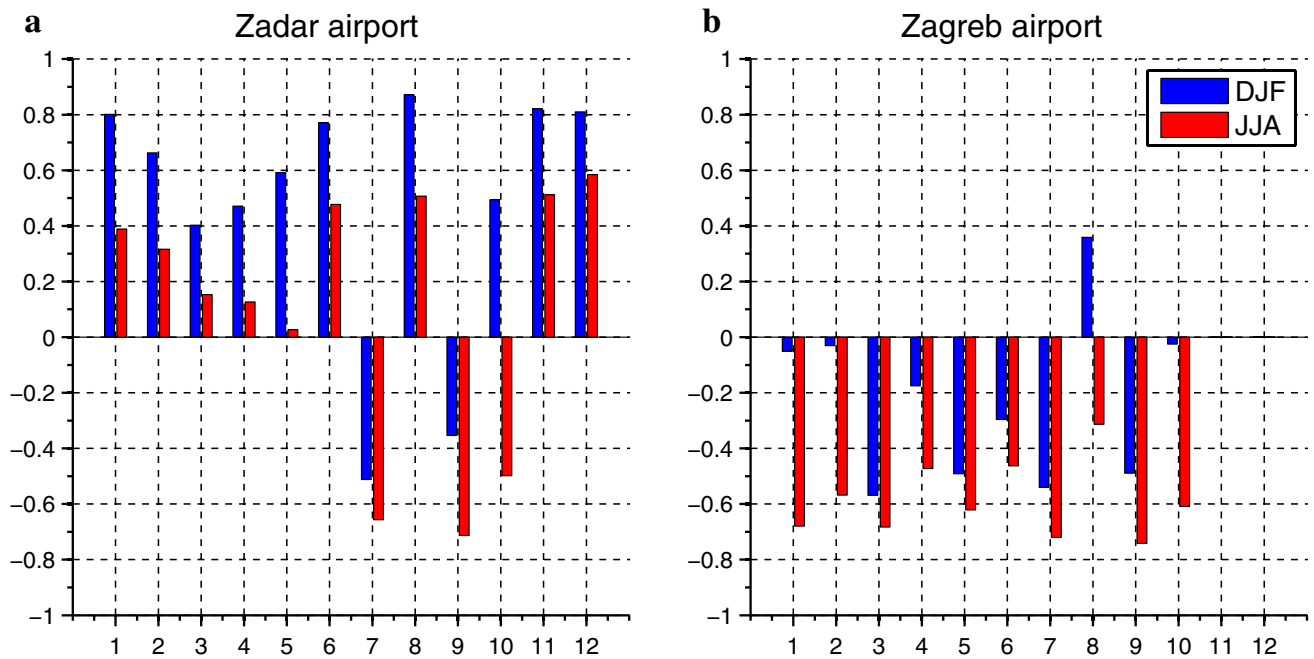


Fig. 9 The modified *BSS* calculated based on ERA-Interim analysis time series for DJF and JJA seasons 0.11° (or 0.02° for ETHZ) simulations using NN technique. **a** coastal station (Zadar airport, 2001–

2008), **b** inland station (Zagreb airport, 1996–2008). Each number at *x*-axis denotes one simulation as in Fig. 3

it overestimates its frequency. The CLM-CCLM CORDEX 0.11° representative simulates the wind magnitude very well, but it overestimates the number of Bora events as well. Similar to ETHZ-CCLM-11, it does not capture the NW flow (i.e., Etesian) correctly. The wind rose is the most sensitive to the very fine topographic changes that can be seen when comparing the CORDEX 0.11° and UPS simulations. The two 0.44° simulations, in principle, both capture Bora, but they overestimate the number of events. The wind rose features greatly change when upscaling is applied, and the discrepancies compared to the observed wind rose are greater than in the corresponding 0.11° simulation. The upscaled simulation also has a slightly higher wind speed. ERA-Interim cannot capture the large variability in the wind field (seen also from Fig. 4c) and it performs similar to the 0.44° CORDEX simulation. Furthermore, for inland stations, no such strong wind events are observed (as seen from the ETHZ simulation in Fig. 2), and therefore, the wind direction frequencies are more evenly distributed. Thus, the coarse-resolution RCMs can, for inland stations, simulate the wind rose (in terms of both direction and speed) more skilfully. While not shown here we would like to add that in other locations greatly influenced by Bora (e.g., Trieste, Split, Dubrovnik (Fig. 2); Prtenjak et al. 2010a; Horvath et al. 2011), all simulations can capture the Bora flow during the period examined.

The strongest Bora events are usually detected in winter (DJF season), particularly at the Senj station (Fig. 2). Here, the observations agree quite well with the RCM simulations [0.11° representative (Fig. 12 b), 0.44° representative (Fig. 12d) and upscaled resolution representative (Fig. 12c)]. The maximum Bora wind speed observed at Senj station is 17 m/s, while the 0.11° simulation gives a maximum of 19 m/s, 0.44° gives 16.5 m/s and the upscaled resolution 12.5 m/s. The NE direction of the Bora wind is captured best by the 0.11° simulation, but overall it shows a low frequency of SE winds not present in the observations. The upscaled simulations and those with 0.44° grid spacing show similar results, underestimating the magnitude and the number of Bora events at Senj. ERA-Interim agrees well with the observations, in terms of both wind direction and magnitude. This is because the wind at this location is persistent during the year (see Sect. 3.1). If the large-scale circulation is captured well, the wind field at this location will also be well represented.

To confirm the results of the wind rose analysis and those of the 2D Kolmogorov–Smirnov test, the study has been complemented by an EOF analysis. In Fig. 13, we present the major axis ratio and major axis angle differences. The simulations that perform well have a simulation/measurement major axis variance ratio close to 1. At open-ocean (Fig. 13a) the observed major axis (which indicates the direction with the most variable wind magnitude) tilt is 158° ,

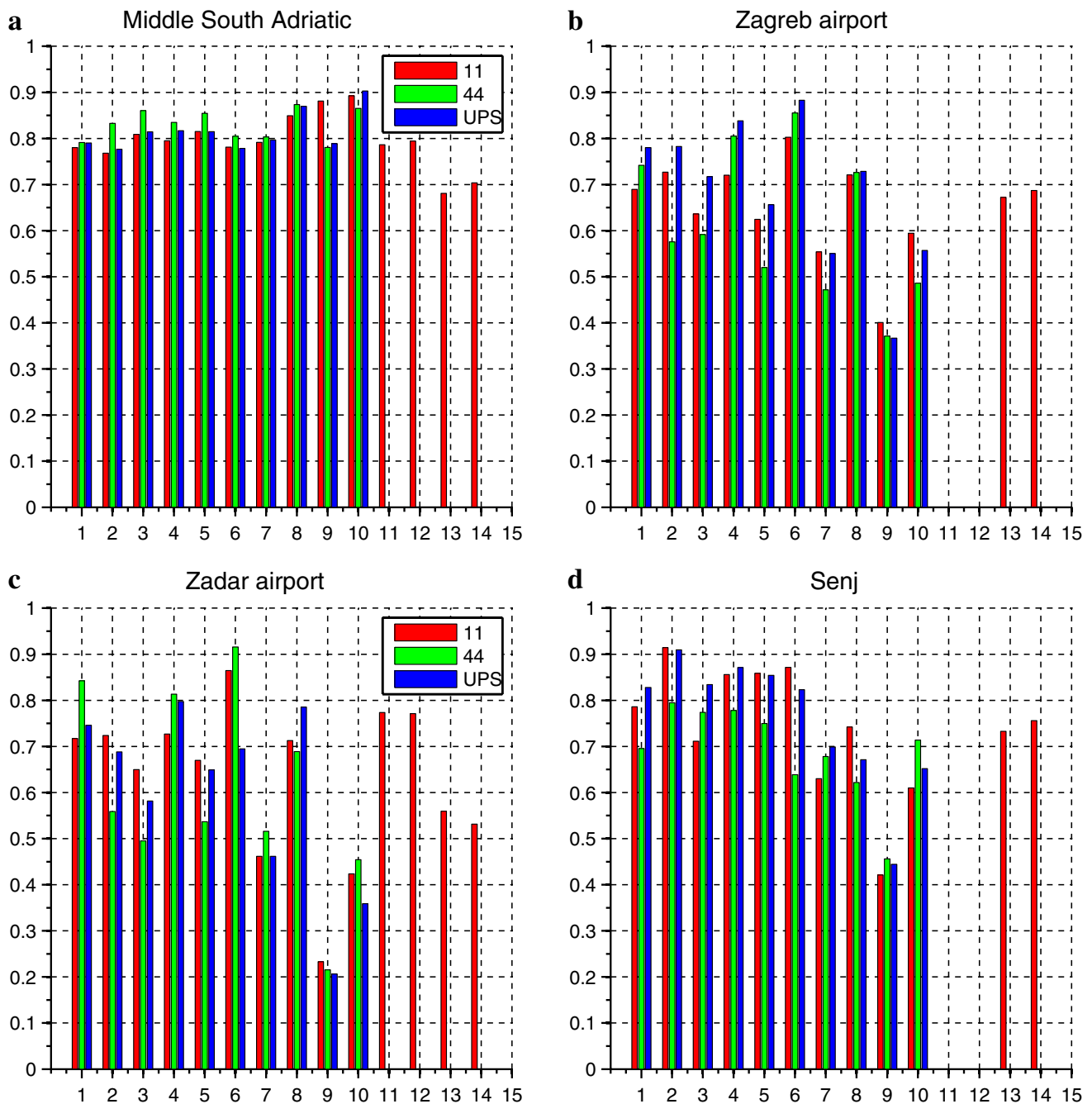


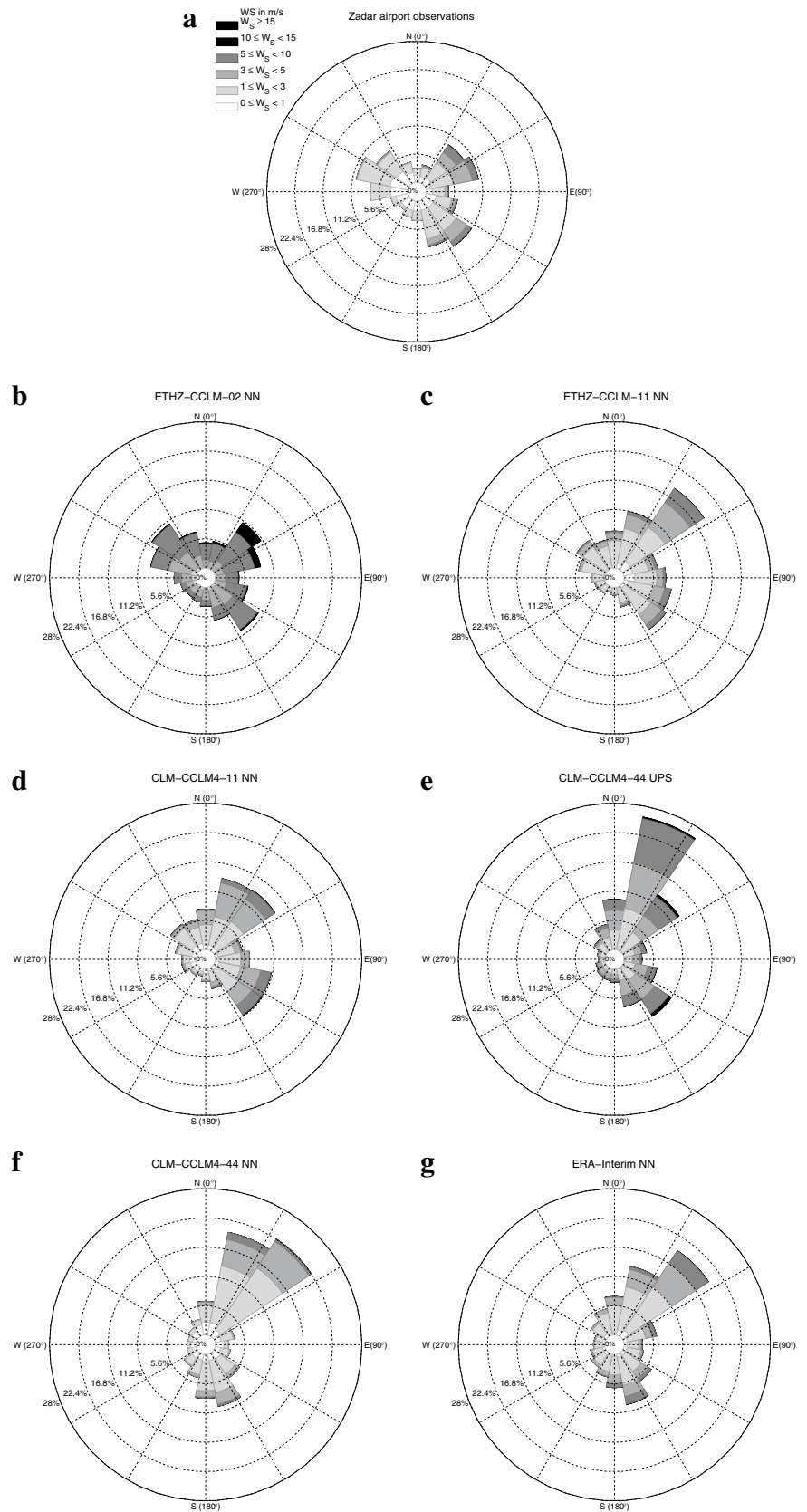
Fig. 10 PSS based on 0.11° (and 0.02°) simulations using NN approach for **a** open-sea location (*Middle South Adriatic*), **b** inland station (Zagreb airport), **c** station in the flat coastal terrain (Zadar airport) and **d** station in the complex coastal terrain (Senj). Each number represents one model as in Fig. 3. Three bars are attached to a single

number representing 0.11° simulation, 0.44° simulation and upscaled 0.11° simulation. ETHZ simulations (when available) have only 0.11° and 0.02° resolution. The period studied: **a, c** 2001–2008, **b, d** 1996–2008

indicating that the NW-SE axis is the most variable. This is because Etesian and Sirocco flows dominate in this region. The ETHZ simulations in Fig. 2b successfully reproduce the JJA Etesian with large persistence. The SE direction corresponds to Sirocco, but we find that it is mostly missing in the

simulations. It can be seen that the discrepancies between the simulations and the measurement are not large overall but are the largest for Zadar airport (Fig. 13c), since this station has a very variable wind direction (see Fig. 11). The angle of the major axis, however, has a shift. At the stations

Fig. 11 Wind rose obtained by NN approach at Zadar airport (2001–2008) for **a** measurements, **b** ETHZ-CCLM-02, **c** ETHZ-CCLM-11, **d** CLM-CCLM4-11, **e** CLM-CCLM4-UPS, **f** CLM-CCLM4-44 and **g** ERA-Interim reanalysis



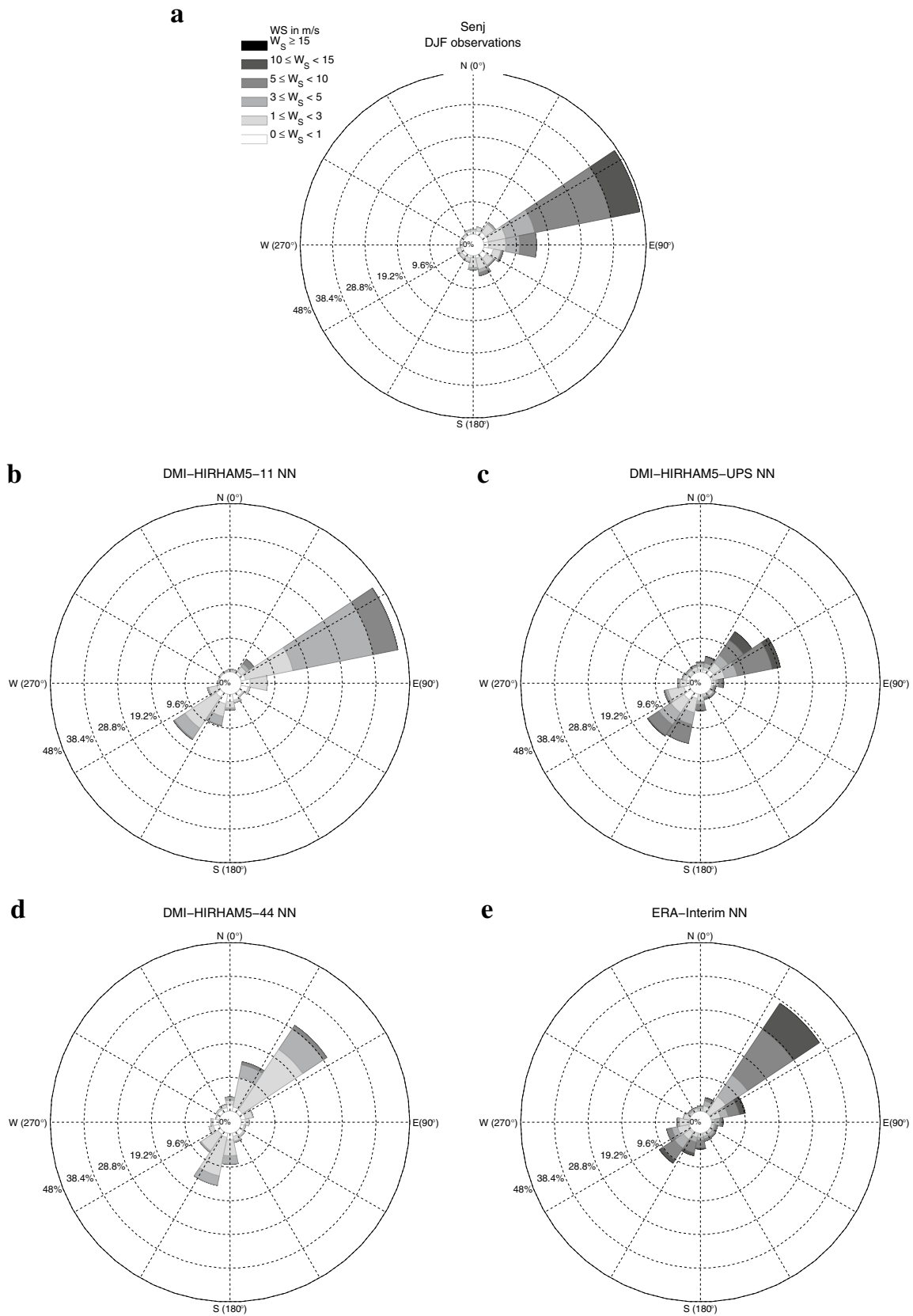


Fig. 12 DJF wind rose obtained by NN approach at Senj (1996–2008) for **a** measurements, **b** DMI-HIRHAM5-11, **c** DMI-HIRHAM-UPS, **d** DMI-HIRHAM5-44 and **e** ERA-Interim reanalysis

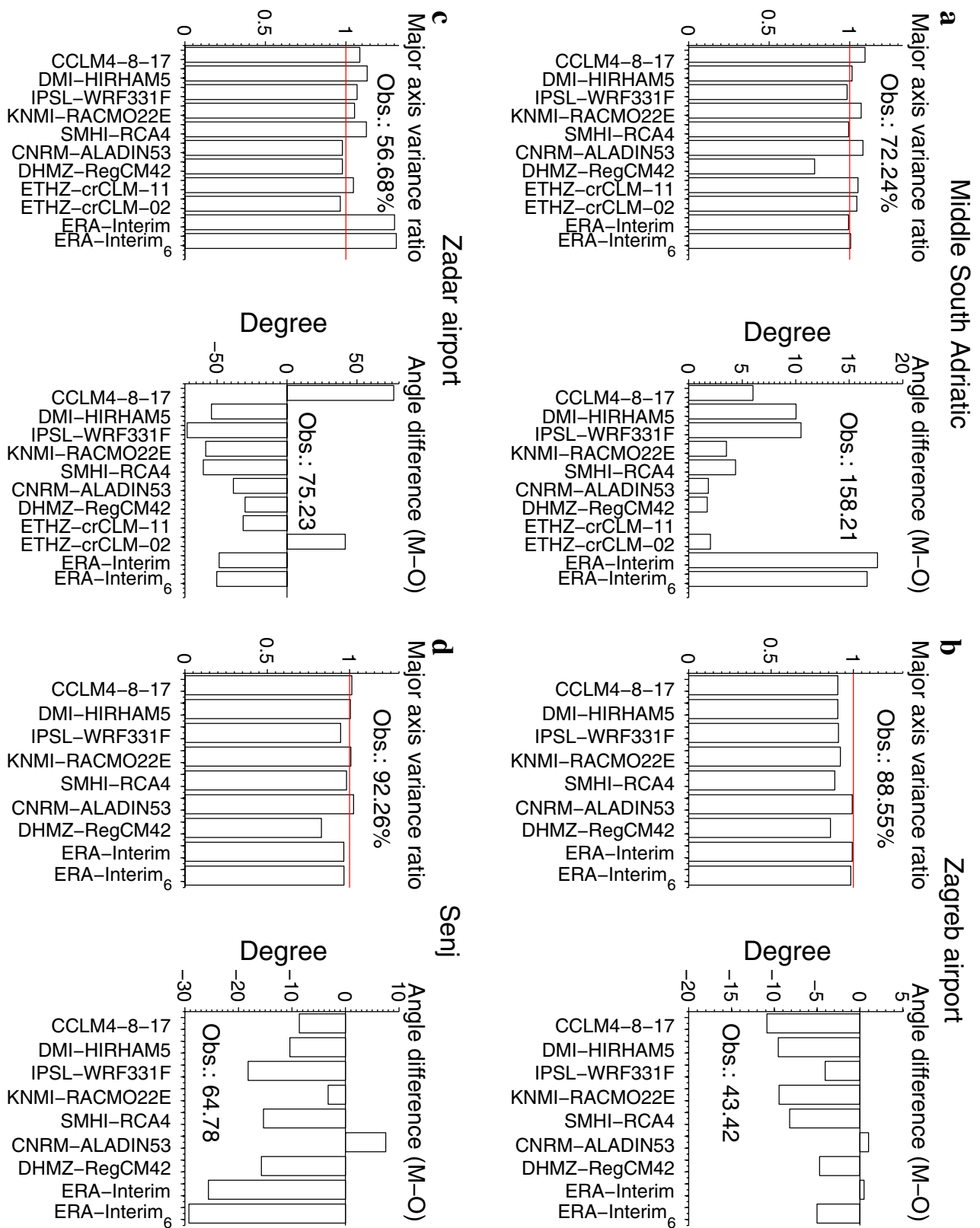


Fig. 13 EOF analysis results for 0.11° simulations; major axis variance ratio (*left*) and major axis angle tilt difference (model-observations) (*right*). Each *x*-axis tick denotes one NN simulation. **a** Middle South Adriatic (open-sea location, 2001–2008), **b** Zagreb airport

(inland location, 1996–2008), **c** Zadar airport (location in the flat coastal terrain, 2001–2008), **d** Senj (location in the complex coastal terrain, 1996–2008)

in the northern part of our domain, both simulations and observations usually have the major axis in the 1st quadrant (NE direction), with the simulations having a tilt shift within the 1st quadrant. The observed tilt changes from north (Senj, where the tilt is 65°) to south (Middle South Adriatic, where the tilt is 158°), and it moves from the NE direction (Bora) to the NW-SE direction (Etesian and Sirocco). The simulations follow that pattern quite well. To corroborate these results further, a denser observational network and more stations with an uninterrupted series of SYNOP data over the southern Adriatic are needed. Another finding of the EOF analysis worth noting is that the RCM simulations can reproduce the climatology of the wind direction, simulating Bora in the north and the Etesian wind in the south Adriatic. This is particularly important because the Bora wind has a large spatial variability in magnitude along the eastern Adriatic coast (Grisogono and Belušić 2009), also shown in Fig. 2.

3.2.4 Spectral analysis

A successful RCM should resemble the power spectrum density function obtained from measurements for the entire

frequency range. To cover the relevant frequency range (i.e., daily and sub-daily scales), power spectrum analysis is considered only for the high-resolution simulations that provide sub-daily data for our study, namely, SMHI-RCA4, DHMZ-RegCM42, ETHZ-CCLM-11 and ETHZ-CCLM-02. No significant differences between the NN and BI approaches were noticed; therefore only the NN time series are shown here. The analysis was performed for stations with less than 10% of SYNOP data missing (c.f. Sect. 2.5). The group representative stations presented above did not fulfil this condition at the sub-daily timescale, so we take another set of stations. Available simulations for Daruvar (Croatia, Fig. 14a), Gospić (Croatia, Fig. 14b), Varaždin (Croatia, Fig. 14c), Zadar airport (Croatia, Fig. 14d), Cervia airport (Italy, Fig. 14e) and Zagreb Maksimir (Croatia, Fig. 14f) disclose three pronounced peaks at 24, 12 and 8 h periods (Ray and Poulou 2005) (Figs. 14, 15), perfectly matching the three peaks present in the observational time series. We notice larger differences between observations and simulations for periods less than 24 h, again implying that the simulations represent large-scale circulation quite well, but the 0.11° simulations have difficulties in simulating motions on a

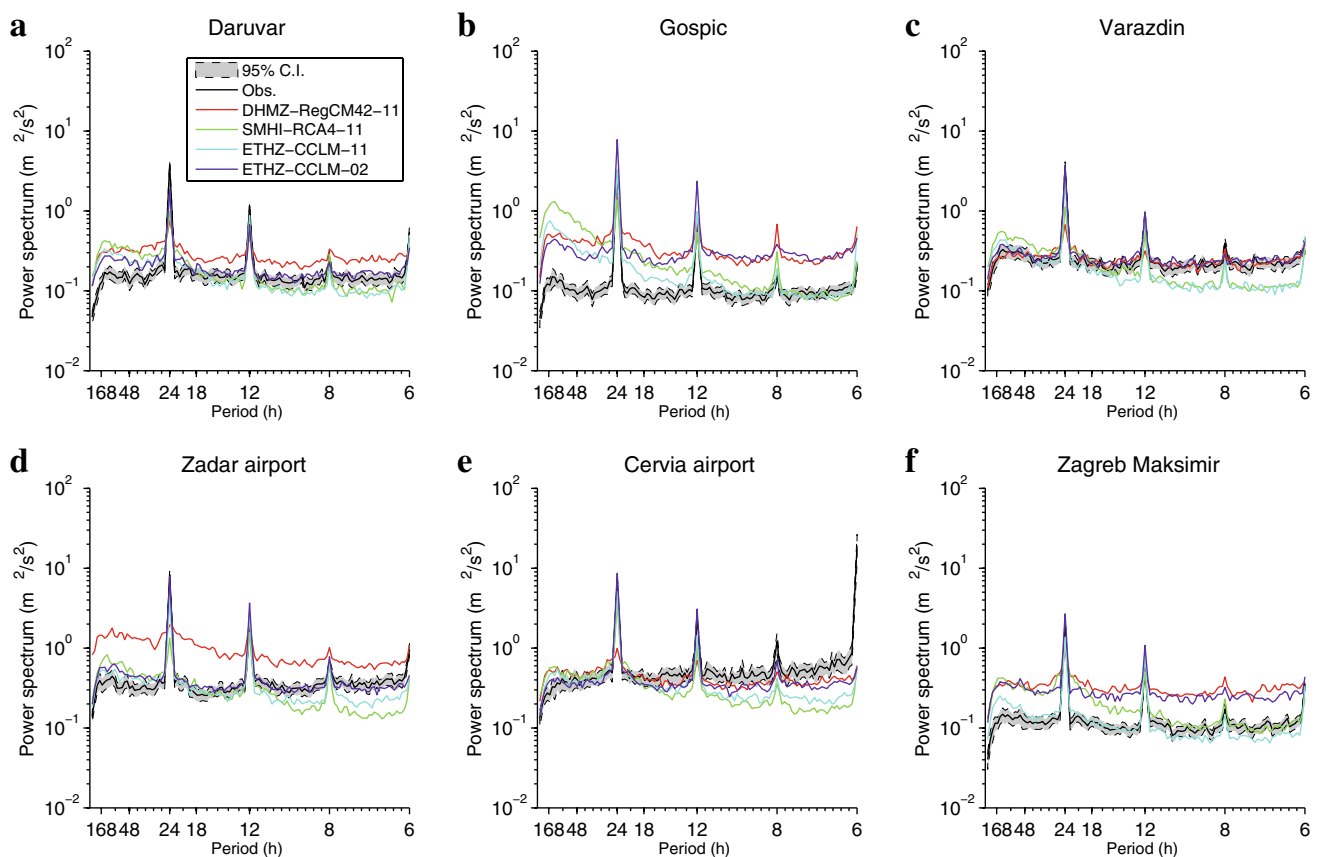


Fig. 14 Observed versus modelled spectral power distribution for wind magnitude at stations: **a** Daruvar (Croatia), **b** Gospić (Croatia), **c** Varaždin (Croatia), **d** Zadar airport (Croatia), **e** Cervia airport (Italy) and **f** Zagreb Maksimir (Croatia). Locations of the stations can

be seen in Fig. 1. The period studied: 2001–2008. Legend in **a** corresponds to all other subfigures; DHMZ-RegCM42-11 in red, SMHI-RCA4-11 in green, ETHZ-CCLM-11 in blue and ETHZ-CCLM-02 in purple

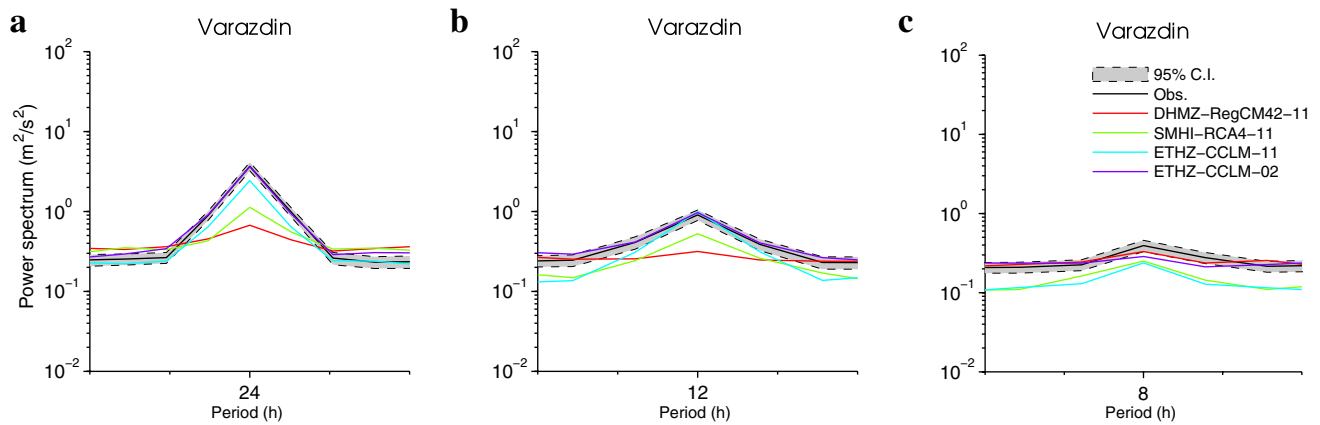


Fig. 15 Spectral power distribution as a function of frequency at Varaždin station (Croatia). The three panels denote zooms into the three prominent energy peaks found in the analysis displayed in Fig. 14. The legend is the same as in Fig. 14

sub-diurnal time scale. For periods less than 24 h, the energy stored in the simulations is more dispersed. The DHMZ-RegCM42 simulation has the greatest energy, while ETHZ-CCLM-02 best fits the observations. Here, we can address the sub-daily differences between the ETHZ-CCLM-11 and ETHZ-CCLM-02 simulations. Both simulations are very close to the observations in the larger-than-diurnal time range, but in the sub-daily time range, the 0.02° simulation agrees better with the observations, having more skill in reproducing features on shorter time scales. Additionally, increasing the horizontal resolution adds more detail, particularly in the maximum wind speed (Figs. 11, 12), but the basic structure remains the same. Consequently, the simulated power is modified, but the positions of the peaks in the spectra do not change (Fig. 15). Figure 15 displays a zoomed illustration for Varaždin station, where ETHZ-CCLM-02 agrees best with the observations and DHMZ-RegCM42 has

the largest discrepancies. Note that the differences between the 0.11° and 0.02° ETHZ simulations are clearly visible, especially for periods less than 24 h (similar to the precipitation and temperature analysed in Ban et al. 2014, 2015).

The spectral power distribution at different ranges, normalized by total power (x-axis) and by the observed power in the same frequency range (y-axis) (following Žagar et al. 2006), is provided in Fig. 16. This figure summarizes information about the spectral power distribution at different time ranges for all 6 stations. Each station is denoted by one symbol, while the colours represent each simulation, as in Fig. 14. The ranges are defined to capture the longer-than-day (LTD, greater than 26 h), diurnal (from 22 to 26 h) and sub-diurnal (6–22 h) motions. All simulations close to the red line and simultaneously close to the corresponding black symbol are considered successful. Looking at the x-axis, we notice that all simulations have more power in the LTD

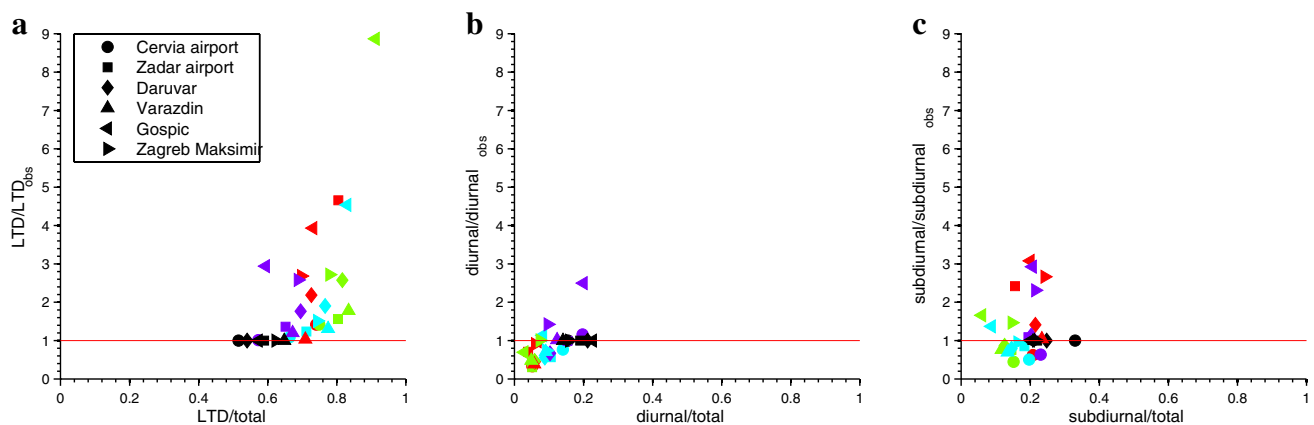


Fig. 16 Spectral wind power at each station in the **a** longer than diurnal (LTD, larger than 26 h), **b** diurnal (from 22 to 26 h) and **c** sub-diurnal (from 6 to 22 h) range normalized by the spectral power in the same frequency range in observations, plotted against the power in a particular spectral range normalized by the total power at specific station. The simulation is considered as successful if it is close

to the red line and at the same time close to the corresponding black symbol. Figure legend associates symbols with various stations, while colours are associated with specific model as in Fig. 14; DHMZ-RegCM42-11 in red, SMHI-RCA4-11 in green, ETHZ-CCLM-11 in blue and ETHZ-CCLM-02 in purple

range than in the diurnal or sub-diurnal ranges (also found in Zagar et al. 2006 and Horvath et al. 2011), meaning that synoptic and longer timescale perturbations contribute over 60% of the spectral power. Hence, the diurnal range is not significant except in the observations (i.e., all simulations have too much power in the LTD range). Looking at the y-axis, all simulations in the LTD range have energy close to or greater than that observed (red line). For diurnal and sub-diurnal motions, there is a large spread under and over the red line, respectively. The simulated LTD spectral power can be close to the observations, but at the same time, it can hold 90% of the total simulated spectral power, which implies that only the LTD range is simulated well and the diurnal and sub-diurnal parts of the spectrum are lacking energy. Let us further investigate the Cervia airport station (Italy), denoted by a circle in Fig. 16. For this site, there is quite a large percentage (compared to other simulations) of sub-diurnal power in ETHZ-CCLM-02; 24% of the simulated power is in the sub-diurnal range, but this represents 52% of the observed sub-diurnal power at this location. The ratio between all simulated and observed power in the LTD range at Cervia airport is almost exactly 1, but the respective values range in their contribution to the total power, from 58% for ETHZ-CCLM-02 to 75% for SMHI-RCA4 and 51% for the observations (Fig. 14), implying that there is a different energy distribution among the subranges in different simulations.

4 Summary and conclusions

In this study, the wind field from RCM simulations over the Adriatic region was extensively evaluated on climate time-scales. For this purpose, all CORDEX simulations, available at the time this study was performed, and two additional simulations provided by ETHZ were employed, as well as a number of methods of model validation.

Here we summarize the main points addressed in this study, and provide an overview of the conclusions.

The simulations with 0.11° and 0.02° grid spacing can realistically simulate important structures of the flow not present in the coarser grid simulations. There is a possibility of added value in the upscaled 0.11° simulations when compared to the 0.44° partners. This is indicated e.g., by the better agreement of the upscaled simulations in terms of the median and the interquartile range of the wind magnitude seen in the boxplots for the representative locations. However, for the modified *BSS*, there is no clear improvement when increasing the grid spacing from 0.44° to 0.11° . At the same time, the default 0.11° and upscaled 0.11° simulations tend to have a slightly higher *PSS* than the corresponding 0.44° simulations.

Differences between the ETHZ simulations at 0.11° and 0.02° can be seen when looking at the sub-daily scale in spectral analysis, where the 0.02° simulations lie within the observational uncertainties.

More details in the spatial structure of the 10 m wind are present as the grid spacing decreases. This is accompanied by more intensive wind in parts of the domain where e.g., Bora wind is a dominant type of flow. Although ERA-Interim has a larger temporal correlation coefficient than all CORDEX RCMs, the temporal correlation coefficient obtained from the ETHZ simulations is similar to ERA-Interim. There might be several reasons for this difference. First, the refinement in grid spacing may not lead to linear improvements in statistical parameters. Second, ERA-Interim assimilates the measurements, but the coarse grid spacing does not permit the evolution of the small-scale events (large *RMSD* for coastal stations). On the other hand, the ETHZ-CCLM-02 simulation, with very fine spatial and temporal resolution, coherently resolves day-to-day events. Since the modified *BSS* is also dependent on the temporal coherence of the events, the majority of the RCMs cannot outperform ERA-Interim in terms of the modified *BSS* (e.g., Senj, where the wind is persistent and is mainly generated by the large-scale circulation).

The results for ERA-Interim are more sensitive to the horizontal interpolation technique than to the differences between the ERA-Interim pure analysis product and the prognostic product. In some cases, (e.g., Taylor diagram), the upscaling of the 0.11° simulations to 0.44° does not introduce major differences in the results and conclusions, while in the QQ plots, the improvements are clearly visible. The choice of interpolation method has the secondary effect on the QQ plots over the entire range of values. However, there are examples where the use of a specific interpolation method can improve the results (e.g., a 30% increase in the modified *BSS* when the interpolation changes from the BI to NN for the ETHZ models for the Zadar airport station).

We document several results that favour specific models. Biases in the wind magnitude are the lowest for the ETHZ simulations and for CNRM-ALADIN53, while the largest biases are found for DHMZ-RegCM42 and ICTP-RegCM43. CNRM-ALADIN53 is generally the best CORDEX model in capturing the observed temporal variability. Even greater improvements are found for the two non-CORDEX simulations, i.e., ETHZ-CCLM-11 and ETHZ-CCLM-02. Also, over the analysed open-sea location, the CNRM-ALADIN53 and ETHZ simulations are better than the ERA-Interim reanalysis, as measured in terms of the modified *BSS*. It is important to keep in mind that discrepancies between simulations and observed data may also be due to inaccuracies in both land-based and QuikSCAT data.

Over the open-sea/inland locations, the models typically underestimate/overestimate the observed wind speed. The

temporal correlation coefficient has a higher value over the open-sea and for steep coastline locations. The observed differences between inland and coastline stations are well captured by the models, with maximum wind speeds over the Adriatic coast dropping when moving inland. The open-sea and inland stations are found to have a smaller ensemble spread (and are grouped around the 1–1 diagonal in the QQ plots) in comparison with the flat coastal stations, where a large ensemble spread and the overestimation of the small wind speed prevails. Also, all models perform fairly well in reproducing the observed PDE of the wind magnitude, as measured by the *PSS*.

Regions of the NE wind with greater speed in the DJF season overlapping with the wind steadiness greater than 60% along the eastern Adriatic coast are observed in the ETHZ-CCLM-02 simulation. They are the part of the well-known Bora jets, which are associated with mountain passes. Opposite to the Bora wind, the Sirocco (SE) wind is not easily distinguishable in the 10 m wind climatology. However, the low wind steadiness over the open-sea area in the DJF season (particularly southward from the Middle South Adriatic) points to the occurrence of such a wind type. In the JJA season, the ETHZ-CCLM-02 simulation can successfully reproduce the JJA southern Adriatic Etesian with large persistence. In the northern Adriatic and in the JJA season, the ETHZ-CCLM-02 simulation indicates the detection of thermally induced winds (sea/land breezes and slope winds) that alternate in wind direction within 24 h. The dominant frequencies of these wind regimes can also be seen in the spectral analysis, which discloses three large peaks at 24, 12 and 8 h periods, also seen in the observational time series.

Based only on this study, no simple recommendation can be made concerning the optimal grid spacing when exploring the wind projection for the 21st. However, higher-resolution simulations provide more details, as they reproduce local winds that influence the life and tourism in these areas and have smaller biases. Since these simulations are quite computationally expensive, it may take several years until we have a set of climate projections comparable to those in the CORDEX project. Thus, our future work will explore the wind projections in climate change simulations from the CORDEX archive. We will evaluate the projected climate change signal in comparison to the inter-ensemble spread and the models' systematic deviations from the observations.

Acknowledgements This work has been supported by the ongoing Croatian Science Foundation (HrZZ) projects CARE (no. 2831) and VITCLIC (PKP-2016-06-2975). The authors would like to thank the reviewers for their suggestions, which have helped improve this paper. A primary idea for this research was established on behalf of the past HrZZ project CATURBO (no. 09/151). The work of the ETH group was supported by the Swiss National Science Foundation through the Sinergia grant CRSII2_154486 'crCLIM'. We want to thank Lidija Srncac and Mirta Patarčić for their contribution in performing parts of the DHMZ-RegCM42 simulations. We also thank Anika Obermann

and Bodo Ahrens for providing the QuikSCAT data and to all CORDEX group members for providing useful information. We acknowledge the World Climate Research Programme's Working Group on Regional Climate and, Working Group on Coupled Modelling, the former coordinating body of CORDEX and the responsible panel for CMIP5. We also thank the climate modelling groups (listed in Table 1 of this paper) for producing and making available their model output. We acknowledge the Earth System Grid Federation infrastructure, an international effort led by the U.S. Department of Energy's Program for Climate Model Diagnosis and Intercomparison, the European Network for Earth System Modelling and other partners in the Global Organisation for Earth System Science Portals (GOESSP). Additionally, the simulations used in this work were downloaded from the Med-CORDEX database (<http://www.medcordex.eu>). ERA-Interim data for wind components were obtained from the European Centre for Medium-Range Weather Forecasts (ECMWF) MARS database. The authors acknowledge ECMWF for providing the MARS database account. The observed data used in this study were acquired from NOAA's National Climatic Data Center (<http://www.ncdc.noaa.gov>), DHMZ database and Crocontrol database.

References

- Accadia C, Zecchetto S, Lavagnini A, Speranza A (2007) Comparison of 10-m wind forecasts from a regional area model and QuikSCAT scatterometer wind observations over the Mediterranean Sea. *Mon Wea Rev* 135:1945–1960. doi:10.1175/MWR3370.1
- Baklanov A, Grisogono B (2007) Atmospheric boundary layers: nature, theory and applications to environmental modelling and security. Springer, New York
- Ban N, Schmidli J, Schär C (2014) Evaluation of the convection-resolving regional climate modeling approach in decade-long simulations. *J Geophys Res Atmos* 119:7889–7907. doi:10.1002/2014JD021478
- Ban N, Schmidli J, Schär C (2015) Heavy precipitation in a changing climate: does short-term summer precipitation increase faster? *Geophys Res Lett* 42:1165–1172. doi:10.1002/2014GL062588
- Belušić D, Guttler I (2010) Can mesoscale models reproduce meandering motions? *QJR Meteorol Soc* 136:553–565. doi:10.1002/qj.606
- Brands S, Herrera S, Fernández J, Gutiérrez JM (2013) How well do CMIP5 earth system models simulate present climate conditions in Europe and Africa? *Clim Dyn* 41:803–817. doi:10.1007/s00382-013-1742-8
- Branković Č, Guttler I, Gajić-Čapka M (2013) Evaluating climate change at the Croatian Adriatic from observations and regional climate models' simulations. *Clim Dyn* 41:2353–2373. doi:10.1007/s00382-012-1646-z
- Cavaleri L, Bertotti L, Tescaro N (1996) Long term wind hindcast in the Adriatic Sea. *Il nuovo cimento C* 19:67–89. doi:10.1007/BF02511834
- Christensen OB, Drews M, Christensen JH, Dethloff K, Ketelsen K, Hebestadt I, Rinke A (2006) The HIRHAM regional climate model, version 5, Tech. Rep. 06–17, Dan Meteorol Inst, Copenhagen. <http://www.dmi.dk/dmi/tr06-17.pdf>. Accessed 21 Sep 2016
- Colin J, Déqué M, Radu R, Somot S (2010) Sensitivity study of heavy precipitations in Limited Area Model climate simulation: influence of the size of the domain and the use of the spectral nudging technique. *Tellus A* 62:591–604. doi:10.1111/j.1600-0870.2010.00467.x
- Dee DP, Uppala SM, Simmons AJ, Berrisford P, Poli P, Kobayashi S, Andrae U, Balmaseda MA, Balsamo G, Bauer P, Bechtold P, Beljaars ACM., Van de Berg L, Bidlot J, Bormann N, Delsol C, Dragani R, Fuentes M, Geer AJ, Haimberger L, Healy SB, Hersbach H, Hólm EV, Isaksen L, Källberg P, Köhler M, Matricardi

- M, McNally AP, Monge-Sanz BM, Morcrette JJ, Park BK, Peubey C, De Rosnay P, Tavolato C, Thépaut JN, Vitart F (2011) The ERA-Interim reanalysis: configuration and performance of the data assimilation system. *QJR Meteorol Soc* 137:553–597. doi:[10.1002/qj.828](https://doi.org/10.1002/qj.828)
- Di Luca A, De Elía R, Laprise R (2015) Challenges in the Queste for added value of regional climate dynamical downscaling. *Curr Clim Change Rep* 1:10–21. doi:[10.1007/s40641-015-0003-9](https://doi.org/10.1007/s40641-015-0003-9)
- Domínguez M, Gaertner MA, De Rosnay P, Losada T (2010) A regional climate model simulation over West Africa: parameterization tests and analysis of land surface fields. *Clim Dyn* 35:249–265. doi:[10.1007/s00382-010-0769-3](https://doi.org/10.1007/s00382-010-0769-3)
- Dunion JP, Landsea CW, Houston SH, Powell MD (2003) A reanalysis of the surface winds for Hurricane Donna of 1960. *Mon Wea Rev* 131:1992–2011. doi:[10.1175/1520-0493\(2003\)131<1992:ARO TSW>2.0.CO;2](https://doi.org/10.1175/1520-0493(2003)131<1992:ARO TSW>2.0.CO;2)
- Feser F, Rockel B, Von Storch H, Winterfeldt J, Zahn M (2011) Regional climate models add value to global model data: a review and selected examples. *B Am Meteorol Soc* 92:1181–1192. doi:[10.1175/2011BAMS3061.1](https://doi.org/10.1175/2011BAMS3061.1)
- Gibbons JD, Chakraborti S (2011) Nonparametric statistical inference, 5th edn. Chapman & Hall/CRC Press, Taylor & Francis Group, Boca Raton, FL
- Giorgi F, Gutowski W Jr (2015) Regional dynamical downscaling and the CORDEX initiative. *Annu Rev Env Resour* 40:467–490. doi:[10.1146/annurev-environ-102014-021217](https://doi.org/10.1146/annurev-environ-102014-021217)
- Giorgi F, Coppola E, Solmon F, Mariotti L, Sylla MB, Bi X, Elguindi N, Diro GT, Nair V, Giuliani G, Cozzini S, Güttler I, O'Brien TA, Tawfik AB, Shalaby A, Zakey AS, Steiner AL, Stordal F, Sloan LC, Branković Č (2012) RegCM4: model description and preliminary tests over multiple CORDEX domains. *Clim Res* 52:7–29. doi:[10.3354/cr01018](https://doi.org/10.3354/cr01018)
- Giorgi F, Csaba T, Coppola E, Ban N, Schär C, Somot S (2016) Enhanced summer convective rainfall at Alpine high elevations in response to climate warming. *Nat Geosci*. doi:[10.1038/ngeo2761](https://doi.org/10.1038/ngeo2761)
- Gómez-Navarro JJ, Raible CC, Dierer S (2015) Sensitivity of the WRF model to PBL parameterisations and nesting techniques: evaluation of wind storms over complex terrain. *Geosci Model Dev* 8:3349–3363. doi:[10.5194/gmd-8-3349-2015](https://doi.org/10.5194/gmd-8-3349-2015)
- Grisogono B, Belušić D (2009) A review of recent advances in understanding the meso- and microscale properties of the severe Bora wind. *Tellus A* 61:1–16. doi:[10.1111/j.1600-0870.2008.00369.x](https://doi.org/10.1111/j.1600-0870.2008.00369.x)
- Güttler I, Stepanov I, Branković Č, Nikulin G, Colin J (2015) Impact of horizontal resolution on precipitation in complex orography simulated by the regional climate model RCA3. *Mon Wea Rev* 143:3610–3627. doi:[10.1175/MWR-D-14-00302.1](https://doi.org/10.1175/MWR-D-14-00302.1)
- Halpern D (1979) Surface wind measurements and low-level cloud motion vectors near the Inter-tropical Convergence Zone in the central Pacific Ocean from November 1977 to March 1978. *Mon Wea Rev* 107:1525–1534
- Heimann D (2001) A model-based wind climatology of the eastern Adriatic coast. *Meteorol Z* 10:5–16. doi:[10.1127/0941-2948/2001/0010-0005](https://doi.org/10.1127/0941-2948/2001/0010-0005)
- Herrmann M, Somot S, Calmanti S, Dubois C, Sevault F (2011) Representation of spatial and temporal variability of daily wind speed and of intense wind events over the Mediterranean Sea using dynamical downscaling: impact of the regional climate model configuration. *Nat Hazards Earth Sys Sci* 11:1983–2001. doi:[10.5194/nhess-11-1983-2011](https://doi.org/10.5194/nhess-11-1983-2011)
- Horvath K, Lin Y-L, Ivančan-Picek B (2008) Classification of cyclone tracks over Apennines and the Adriatic Sea. *Mon Wea Rev* 136:2210–2227. doi:[10.1175/2007MWR2231.1](https://doi.org/10.1175/2007MWR2231.1)
- Horvath K, Bajić A, Ivatek-Šahdan S (2011) Dynamical Downscaling of wind speed in complex terrain prone to bora-type flows. *J Appl Meteorol Clim* 50:1676–1691. doi:[10.1175/2011JAMC2638.1](https://doi.org/10.1175/2011JAMC2638.1)
- Jacob D, Petersen J, Eggert B, Alias A, Christensen OB, Bouwer L, Braun A, Colette A, Déqué M, Georgievski G, Georgopoulou E, Gobiet A, Menut L, Nikulin G, Haensler A, Hempelmann N, Jones C, Keuler K, Kovats S, Kröner N, Kotlarski S, Kriegsmann A, Martin E, Van Meijgaard E, Moseley C, Pfeifer S, Preuschmann S, Radermacher C, Radtke K, Rechid D, Rounseve IIM, Samuelsson P, Somot S, Soussana JF, Teichmann C, Valentini R, Vautard R, Weber B, Yiou P (2013) EURO-CORDEX: new high-resolution climate change projections for European impact research. *Regl Environ Change* 14:563–578. doi:[10.1007/s10113-013-0499-2](https://doi.org/10.1007/s10113-013-0499-2)
- Kotlarski S, Keuler K, Christensen OB, Colette A, Déqué M, Gobiet A, Goergen K, Jacob D, Lüthi D, Van Meijgaard E, Nikulin G, Schär C, Teichmann C, Vautard R, Warrach-Sagi K, Wulfmeyer V (2014) Regional climate modeling on European scales: a joint standard evaluation of the EURO-CORDEX RCM ensemble. *Geosci Model Dev* 7:1297–1333. doi:[10.5194/gmd-7-1297-2014](https://doi.org/10.5194/gmd-7-1297-2014)
- Leutwyler D, Fuhrer O, Lapillonne X, Lüthi D, Schär C (2016) Towards European-scale convection-resolving climate simulations. *Geosci Model Dev* 9:3393–3412. doi:[10.5194/gmd-2016-119](https://doi.org/10.5194/gmd-2016-119)
- Leutwyler D, Lüthi D, Ban N, Fuhrer O, Schär C (2017) Evaluation of the convection-resolving climate modeling approach on continental scales. *J Geophys Res Atmos* 122:5237–5258. doi:[10.1002/2016JD026013](https://doi.org/10.1002/2016JD026013)
- Ludwig FL, Horel J, Whiteman CD (2004) Using EOF analysis to identify important surface wind patterns in mountain valleys. *J Appl Meteorol* 43:969–983. doi:[10.1175/1520-0450](https://doi.org/10.1175/1520-0450)
- Mayer S, Fox Maule C, Sobolowski S, Christensen OB, Sorup HJD, Sunyer MA, Arnbjerg-Nielsen K, Barstad I (2015) Identifying added value in high-resolution climate simulations over Scandinavia. *Tellus A* 67:1–18. doi:[10.3402/tellusa.v67.24941](https://doi.org/10.3402/tellusa.v67.24941)
- Menendez M, García-Díez M, Fita L, Fernández J, Méndez FJ, Gutiérrez JM (2014) High-resolution sea wind hindcasts over the Mediterranean area. *Clim Dyn* 42:1857–1872. doi:[10.1007/s00382-013-1912-8](https://doi.org/10.1007/s00382-013-1912-8)
- Obermann A, Bastin S, Belamari S, Conte D, Gaertner MA, Li L, Ahrens B (2016) Mistral and Tramontane wind speed and wind direction patterns in regional climate simulation. *Clim Dyn* 47:1–18. doi:[10.1007/s00382-016-3053-3](https://doi.org/10.1007/s00382-016-3053-3)
- Pasarić M, Orlić M (2004) Meteorological forcing of the Adriatic: present vs. projected climate conditions. *Geofizika* 21:69–87
- Pašičko R, Branković Č, Šimić Z (2012) Assessment of climate change impacts on energy generation from renewable sources in Croatia. *Renew Energy* 46:224–231. doi:[10.1016/j.renene.2012.03.029](https://doi.org/10.1016/j.renene.2012.03.029)
- Peacock JA (1983) Two-dimensional goodness-of-fit testing in astronomy. *Mon Not R Astron Soc* 202:615–627. doi:[10.1093/mnras/202.3.615](https://doi.org/10.1093/mnras/202.3.615)
- Perkins SE, Pitman AJ, Holbrook NJ, McAneney J (2007) Evaluation of the AR4 climate models' simulated daily maximum temperature, minimum temperature, and precipitation over Australia using probability density functions. *J Clim* 20:4356–4376. doi:[10.1175/JCLI4253.1](https://doi.org/10.1175/JCLI4253.1)
- Perry KL (2001) Sea winds on QuikSCAT level 3 daily, gridded Ocean wind vectors (JPL Sea Winds Project) version 1.1. (JPL Document D-20335). Jet Propulsion, Pasadena, CA
- Pielke RA (2002) Mesoscale meteorological modeling. Academic, USA
- Poje D (1992) Wind persistence in Croatia. *Int J Climatol* 12:569–586. doi:[10.1002/joc.3370120604](https://doi.org/10.1002/joc.3370120604)
- Powell MD, Houston SH, Ares I (1995) Real-time damage assessment in hurricanes. Preprints, 21st Conf. on Hurricanes and Tropical Meteorology, Miami, FL, Amer. Meteor. Soc., pp 500–502
- Prein AF, Langhans W, Fosser G, Ferrone A, Ban N, Goergen K, Keller M, Tille M, Gutjahr O, Feser F, Brisson E, Kollet S, Schmidli J, van Lipzig NPM, Leung R (2015) A review on regional convection-permitting climate modeling: demonstrations, prospects,

- and challenges. *Rev Geophys* 53:323–361. doi:[10.1002/2014RG000475](https://doi.org/10.1002/2014RG000475)
- Prein AF, Gobiet A, Truhetz H, Keuler K, Goergen K, Teichmann C, Fox Maule C, Van Meijgaard E, Déqué M, Nikulin G, Vautard R, Colette A, Kjellström E, Jacob D (2016) Precipitation in the EURO-CORDEX 0.11° and 0.44° simulations: high resolution, high benefits? *Clim Dyn* 46:383–412. doi:[10.1007/s00382-015-2589-y](https://doi.org/10.1007/s00382-015-2589-y)
- Prtenjak MT, Tomažič I, Kavčič I, Đivanović S (2010a) Characteristics of shallow thermally driven flow in the complex topography of the south-eastern Adriatic. *Ann Geophys* 28:1905–1922. doi:[10.5194/angeo-28-1905-2010](https://doi.org/10.5194/angeo-28-1905-2010)
- Prtenjak MT, Viher M, Jurković J (2010b) Sea-land breeze development during a summer Bora event along the north-eastern Adriatic coast. *QJR Meteorol Soc* 136:1554–1571. doi:[10.1002/qj.649](https://doi.org/10.1002/qj.649)
- Prtenjak MT, Horvat I, Tomažič I, Kvakić M, Viher M, Grisogono B (2015) Impact of mesoscale meteorological processes on anomalous radar propagation conditions over the northern Adriatic area. *J Geophys Res* 120:8759–8782. doi:[10.1002/2014JD022626](https://doi.org/10.1002/2014JD022626)
- Pryor SC, Nikulin G, Jones C (2012) Influence of spatial resolution on regional climate model derived wind climates. *J Geophys Res* 117:D03117. doi:[10.1029/2011JD016822](https://doi.org/10.1029/2011JD016822)
- Ranjha R, Tjernström M, Svensson G, Semedo A (2016) Modelling coastal low-level wind-jets: does horizontal resolution matter? *Meteorol Atmos Phys* 128:263–278. doi:[10.1007/s00703-015-0413-1](https://doi.org/10.1007/s00703-015-0413-1)
- Ray RD, Poulou S (2005) Terdiurnal surface–pressure oscillations over the Continental United States. *Mon Wea Rev* 133:2526–2534. doi:[10.1175/MWR2988.1](https://doi.org/10.1175/MWR2988.1)
- Rockel B, Will A, Hense A (2008) The regional climate model COSMO-CLM (CCLM). *Meteorol Z* 17:347–348. doi:[10.1127/0941-2948/2008/0309](https://doi.org/10.1127/0941-2948/2008/0309)
- Rummukainen M (2010) State-of-the-art with regional climate models. *WIREs Clim Change* 1:82–96. doi:[10.1002/wcc.8](https://doi.org/10.1002/wcc.8)
- Rummukainen M (2016) Added value in regional climate modeling. *WIREs Clim Change* 7:145–459. doi:[10.1002/wcc.378](https://doi.org/10.1002/wcc.378)
- Ruti PM, Marullo S, D'Ortenzio F, Tremant M (2008) Comparison of analysed and measured wind speeds in the perspective of oceanic simulations over the Mediterranean basin: analyses, QuikSCAT and buoy data. *J Mar Syst* 70:33–48. doi:[10.1016/j.jmarsys.2007.02.02640](https://doi.org/10.1016/j.jmarsys.2007.02.02640)
- Ruti PM, Somot S, Giorgi F, Dubois C, Flaouanas E, Obermann A, Dell'Aquila A, Pisacane G, Harzallah A, Lombardi E, Ahrens B, Akhtar N, Alias A, Arsouze T, Aznar R, Bastin S, Bartholy J, Béranger K, Beuvier J, Bouffies-Cloché S, Brauch J, Cabos W, Calmanti S, Calvet J, Carillo A, Conte D, Coppola E, Djurdjevic V, Drobinski P, Elizalde-Arellano A, Gaertner M, Galàn P, Gallardo C, Gualdi S, Goncalves M, Jorba O, Jordà G, L'Heveder B, Lebeaupin-Brossier C, Li L, Liguori G, Lionello P, Maciàs D, Nabat P, Önol B, Raikovic B, Ramage K, Sevault F, Sannino G, Struglia MV, Sanna A, Torma C, Vervatis V (2016) Med-CORDEX initiative for Mediterranean climate studies. *B Am Meteorol Soc* 97:1187–1208. doi:[10.1175/BAMS-D-14-00176.1](https://doi.org/10.1175/BAMS-D-14-00176.1)
- Samuelsson P, Jones CG, Willén U, Ullerstig A, Gollvik S, Hansson U, Jansson C, Kjellström E, Nikulin G, Wyser K (2011) The Rossby Centre regional climate model RCA3: model description and performance. *Tellus A* 63:4–23. doi:[10.1111/j.1600-0870.2010.00478.x](https://doi.org/10.1111/j.1600-0870.2010.00478.x)
- Skamarock W, Klemp J, Dudhia J, Gill D, Barker D, Duda M, Huang X, Wang W, Powers J (2008) A description of the advanced research WRF version 3. Technical Report, NCAR. <http://opensky.ucar.edu/islandora/object/technotes:500>. Accessed 21 Sep 2016
- Smith A, Lott N, Vose R (2011) The integrated surface database: recent developments and partnerships. *B Am Meteorol Soc* 92:704–708. doi:[10.1175/2011BAMS3015.1](https://doi.org/10.1175/2011BAMS3015.1)
- Somot S, Ruti PM; The MedCORDEX team (2011) The Med-CORDEX initiative: towards fully coupled Regional Climate System Models to study the Mediterranean climate variability, change and impact. https://www.medcordex.eu/somot_MedCORDEX_WCRP2011_Denver_oct2011.pdf. Accessed 9 Nov 2016
- Sotillo MG, Ratsimandresy AW, Carretero JC, Bentamy A, Valero F, González-Rouco F (2005) A high-resolution 44-year atmospheric hindcast for the Mediterranean Basin: contribution to the regional improvement of global reanalysis. *Clim Dyn* 25:219–236. doi:[10.1007/s00382-005-0030-7](https://doi.org/10.1007/s00382-005-0030-7)
- Stiperski I, Ivančan-Picek B, Grubišić V, Bajić A (2012) Complex Bora flow in the lee of Southern Velebit. *QJR Meteorol Soc* 138:1490–1506. doi:[10.1002/qj.1901](https://doi.org/10.1002/qj.1901)
- Tang W, Liu WT, Stiles BW (2004) Evaluation of high-resolution ocean surface vector winds measured by QuikSCAT scatterometer in coastal regions. *IEEE Trans Geosci Remote Sens* 42:1762–1769. doi:[10.1109/TGRS.2004.831685](https://doi.org/10.1109/TGRS.2004.831685)
- Taylor KE (2001) Summarizing multiple aspects of model performance in a single diagram. *J Geophys Res Atmos* 106:7183–7192. doi:[10.1029/2000JD900719](https://doi.org/10.1029/2000JD900719)
- Torma C, Giorgi F, Coppola E (2015) Added value of regional climate modeling over areas characterized by complex terrain- Precipitation over the Alps. *J Geophys Res Atmos* 120:3957–3972. doi:[10.1002/2014JD022781](https://doi.org/10.1002/2014JD022781)
- Turuncoglu UU, Sannino G (2016) Validation of newly designed regional earth system model (RegESM) for Mediterranean Basin. *Clim Dyn* 47:1–29. doi:[10.1007/s00382-016-3241-1](https://doi.org/10.1007/s00382-016-3241-1)
- Van Meijgaard E, Van Uft LH, Van De Berg WJ, Bosvelt FC, Van Den Hurk BJM, Lenderink G, Siebesma AP (2008) The KNMI regional atmospheric model RACMO version 2.1, technical report 302. Technical report, De Bilt KNMI, The Netherlands. <http://bibliotheek.knmi.nl/knmipub/TR/TR302.pdf>. Accessed 21 Sep 2016
- Vautard R, Gobiet A, Jacob D, Belda M, Colette A, Déqué M, Fernández J, García-Díez M, Goergen K, Güttler I, Halenka T, Karacostas T, Katragkou E, Keuler K, Kotlarski S, Mayer S, Van Meijgaard E, Nikulin G, Patarčić M, Scinocca J, Sobolowski S, Suklitsch M, Teichmann C, Warrach-Sagi K, Wulfmeyer V, Yiou P (2013) The simulation of European heat waves from an ensemble of regional climate models within the EURO-CORDEX project. *Clim Dyn* 41:2555–2575. doi:[10.1007/s00382-013-1714-z](https://doi.org/10.1007/s00382-013-1714-z)
- Večenaj Ž, Belušić D, Grisogono B (2010) Characteristics of the near-surface turbulence during a Bora event. *Ann Geophys* 28:155–163
- von Storch H, Langenberg H, Feser F (2000) A spectral nudging technique for dynamical downscaling purposes. *Mon Wea Rev* 128:3664–3673. doi:[10.1175/1520-0493\(2000\)128<3664:ASN TFD>2.0.CO;2](https://doi.org/10.1175/1520-0493(2000)128<3664:ASN TFD>2.0.CO;2)
- Weisman M, Skamarock W, Klemp J (1997) The resolution dependence of explicitly modeled convective systems. *Mon Wea Rev* 125:527–548
- Winterfeldt J, Weisse R (2009) Assessment of value added for surface marine wind speed obtained from two regional climate models. *Mon Wea Rev* 137:2955–2965. doi:[10.1175/2009MWR2704.1](https://doi.org/10.1175/2009MWR2704.1)
- Winterfeldt J, Geyer B, Weisse R (2011) Using QuikSCAT in the added value assessment of dynamically downscaled wind speed. *Int J Climatol* 31:1028–1039. doi:[10.1002/joc.2105](https://doi.org/10.1002/joc.2105)
- Žagar N, Žagar M, Cedilnik J, Gregorič G, Rakovec J (2006) Validation of mesoscale low-level winds obtained by dynamical downscaling of ERA40 over complex terrain. *Tellus A* 58:445–455. doi:[10.1111/j.1600-0870.2006.00186.x](https://doi.org/10.1111/j.1600-0870.2006.00186.x)